Bark beetle effects on fire regimes depend on underlying fuel modifications in semiarid systems

Jianning Ren[1], Erin Hanan[1], Jeffrey Hicke[2], Crystal Kolden[3], John T Abatzoglou[4], Christina Tague[5], Ryan Bart[3], Maureen C Kennedy[6], Mingliang Liu[7], and Jennifer Adam[8]

[1]University of Nevada, Reno
[2]University of Idaho
[3]UC Merced
[4]University of California Merced
[5]University of California, Santa Barbara
[6]University of Washington
[7]Unknown
[8]Washington State University

August 8, 2023

Abstract

Although natural disturbances such as wildfire, extreme weather events, and insect outbreaks play a key role in structuring ecosystems and watersheds worldwide, climate change has intensified many disturbance regimes, which can have compounding negative effects on ecosystem processes and services. Recent studies have highlighted the need to understand whether wildfire increases or decreases after large-scale beetle outbreaks. However, observational studies have produced mixed results. To address this, we applied a coupled ecohydrological-fire regime-beetle effects model (RHESSys-WMFire-Beetle) in a semiarid watershed in the western US. We found that surface fire probability and fire size decreased in the red phase (0-5 years post-outbreak), increased in the gray phase (6-15 years post-outbreak), and depended on mortality level in the old phase (one to several decades post-outbreak). In the gray and old phases, surface fire size and probability did not respond to low levels of beetle-caused mortality (<=20%), increased during medium levels of mortality (>20% and <=50%), and remained elevated but did not change with mortality (during the gray phase) or decreased (during the old phase) when mortality was high (>50%). Wildfire responses also depended on fire regime. In fuel-limited locations, fire typically increased with increasing fuel loads, whereas in fuel-abundant (flammability-limited) systems, fire sometimes decreased due to decreases in fuel aridity. This modeling framework can improve our understanding of the mechanisms driving wildfire responses and aid managers in predicting when and where fire hazards will increase.

Bark beetle effects on fire regimes depend on underlying fuel modifications in semiarid systems

[1,2]Jianning Ren, [2]Erin J. Hanan, [3]Jeffrey A. Hicke, [4]Crystal A. Kolden, [4]John T. Abatzoglou, [5]Christina (Naomi) L. Tague, [6]Ryan R. Bart, [7]Maureen C. Kennedy, [1]Mingliang Liu, [1]Jennifer C. Adam

[1] Department of Civil & Environmental Engineering, Washington State University, 99164, Pullman, USA

[2] Department of Natural Resources and Environmental Science, University of Nevada, Reno, 89501, Reno, USA

[3] Department of Geography, University of Idaho, 83844, Moscow, USA

[4] Management of Complex Systems, University of California, Merced, 95343, Merced, USA

[5] Bren School of Environmental Science & Management, University of California, Santa Barbara, 93106, Santa Barbara, USA

[6] Sierra Nevada Research Institute, University of California, Merced, 95343, Merced, USA

[7] School of Interdisciplinary Arts and Sciences, Division of Sciences and Mathematics, University of Washington, Tacoma, 98402, Tacoma, USA

Correspondence:

Jennifer Adam, Department of Civil & Environmental Engineering, Washington State University, PO Box 642910, Pullman, WA 99164-2901, USA (jcadam@wsu.edu)

Abstract

Although natural disturbances such as wildfire, extreme weather events, and insect outbreaks play a key role in structuring ecosystems and watersheds worldwide, climate change has intensified many disturbance regimes, which can have compounding negative effects on ecosystem processes and services. Recent studies have highlighted the need to understand whether wildfire increases or decreases after large-scale beetle outbreaks. However, observational studies have produced mixed results. To address this, we applied a coupled ecohydrologic-fire regime-beetle effects model (RHESSys-WMFire-Beetle) in a semiarid watershed in the western US. We found that surface fire probability and fire size decreased in the red phase (0-5 years post-outbreak), increased in the gray phase (6-15 years post-outbreak), and depended on mortality level in the old phase (one to several decades post-outbreak). In the gray and old phases, surface fire size and probability did not respond to low levels of beetle-caused mortality (<=20%), increased during medium levels of mortality (>20% and <=50%), and remained elevated but did not change with mortality (during the gray phase) or decreased (during the old phase) when mortality was high (>50%). Wildfire responses also depended on fire regime. In fuel-limited locations, fire typically increased with increasing fuel loads, whereas in fuel-abundant (flammability-limited) systems, fire sometimes decreased due to decreases in fuel aridity. This modeling framework can improve our understanding of the mechanisms driving wildfire responses and aid managers in predicting when and where fire hazards will increase.

Plain Language Summary

Bark beetle outbreaks have impacted millions of hectares of forest in western North America. Beetle-caused tree mortality can increase or decrease wildfire hazards by altering surface fuel loading and decreasing leaf moisture. Previous studies have observed increases in fire following beetle attacks. However, others have found no change or decrease. Such discrepancies can result from several interacting factors, such as how much time has passed since an outbreak, the level of tree mortality, and pre-outbreak fuel conditions. To examine how these factors influence fire regimes in a semiarid watershed, we used a model that simulates interactions among hydrology, vegetation, beetle effects, and fire. We found that in the first 5 years after attack, fire probability decreased due to decreases in plant productivity and fuel loading. Following that, fire responses were a function of two counteracting forces: increases in fuel loading from delayed needle- and snag-fall and decreases in fuel aridity from reduced plant water demand. The dominant force depended on fuel conditions. In fuel-limited locations, fire increased with increasing fuel loads, whereas in fuel-abundant locations, fire sometimes decreased due to decreases in aridity. This research provides a tool for managers to better predict when and where fire hazards will increase.

Key Points:

- In five years after beetle outbreaks, fire probability decreased due to reduced vegetation productivity and fuel loading compared to no outbreak scenario.
- In six to fifteen years after outbreak, fire probability increased due to more fuel loading from snag fall.
- Fifteen years after outbreak, fire probability can decrease due to lower fuel aridity when mortality level was larger than 50%.

Key Words: fire regime, beetle outbreaks, fuel loads, fuel aridity, fire severity

1 Introduction

Bark beetle outbreaks and wildfire are significant agents of change in North American forests (Hicke et al., 2012, 2016). In recent decades, these compounding disturbances have increased significantly and affected millions of hectares of forest (Hicke et al., 2016; Littell et al., 2009; Raffa et al., 2008; Seidl et al., 2020). While climate change is expected to continue to increase the severity and frequency of these disturbances, it is less clear how they will interact with one another (Bennett et al., 2018). Bark beetle outbreaks can change fuel conditions and corresponding wildfire characteristics by altering ecohydrological processes and forest fuel structure (Goeking & Tarboton, 2020; Wayman & Safford, 2021). However, the direction of ecohydrological responses to beetle outbreaks can vary over space and time within watersheds (Ren et al., 2021), which can in turn influence fuel loading, fuel moisture, and fire regimes. Therefore, understanding and managing fire risk in landscapes that are prone to these compounding disturbances requires understanding how fuel conditions changes over space and time.

There are three phases of tree response to beetle outbreaks: the red phase, gray phase, and old phase. The "red phase" occurs 0-5 years after beetle outbreak, during which foliar moisture content decreases and some conifer species' needles turn red (Hicke et al., 2012; Jolly, Parsons, Hadlow, et al., 2012). The "gray phase" occurs 6-15 years after beetle outbreak, when dead foliage falls to the ground but snags remain standing (Halofsky et al., 2020). The "old phase" occurs one or more decades after beetle outbreak, when snags fall to ground and the understory vegetation cover increases (Hicke et al., 2012; Mitchell & Preisler, 1998). While, classifying these discrete phases is helpful for understanding post-outbreak processes, their length can vary among tree species, and because beetles can attack trees for multiple years, a mix of different phases can occur in a single stand (Hicke et al., 2012).

Like other ecohydrological processes, fuel conditions and wildfire respond differently to the three phases of beetle outbreak. Hicke et al., (2012) developed a conceptual framework that describes how beetle-caused tree mortality affects wildfire behavior (Figure 1). During the red phase, dead foliage is still in the canopy, thus dead surface fuels remain unchanged, but canopy foliage gets dries out, becoming more flammable. Consequently, surface fire hazard (e.g., the probability of fire and fire severity) remains unchanged but crown fire potential increases. In the gray phase, needle fall increases dead surface fuel loading and reduces canopy bulk density. As a result, surface fire hazard and severity increase but crown fire potential decreases. In the old phase, as dead snags fall to the ground and understory vegetation cover increases, surface fire hazard and severity remains elevated, while crown fire potential may further decrease with decreasing canopy bulk density.

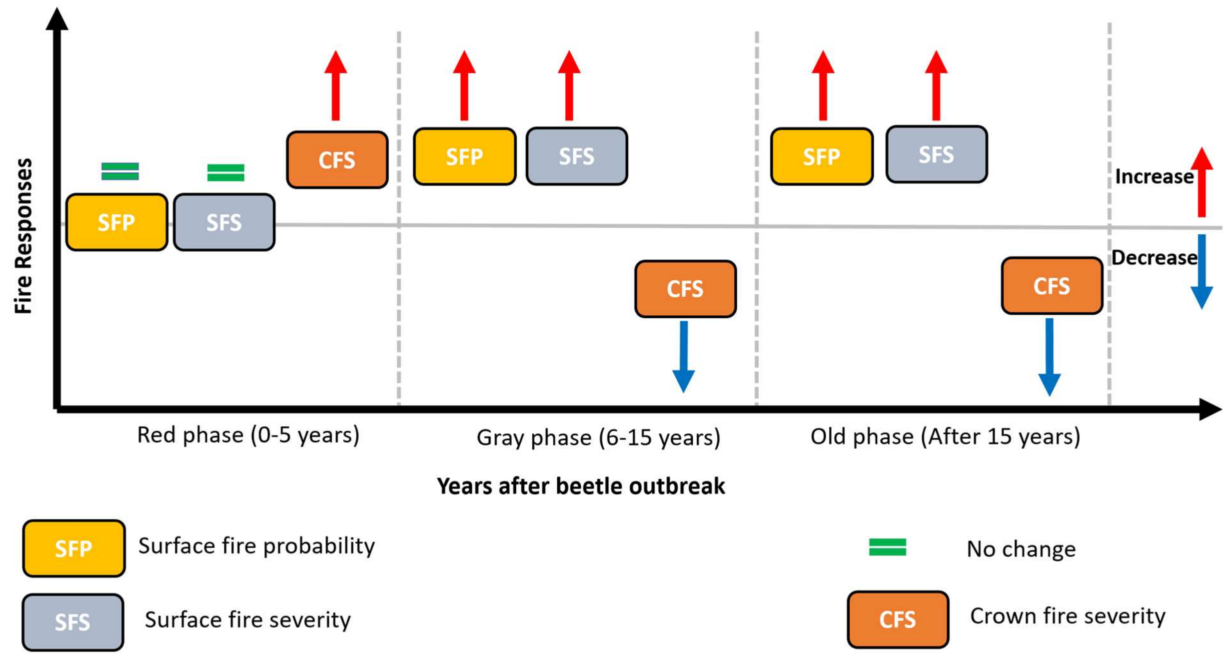

Figure 1. Conceptual framework of wildfire responses to beetle outbreaks adapted from Hicke et al. (2012). A summary of mechanisms is described in Table S1.

While the conceptual framework outlined above is useful for understanding temporal wildfire responses to beetle outbreaks, several uncertainties still remain (Halofsky et al., 2020; Hicke et al., 2012). For example, in the gray and old phases, many studies have documented a decrease or no change of fire probability and fire severity (Ager et al., 2007; Bebi et al., 2003; Berg et al., 2006; Lundquist, 2007; Lynch et al., 2006; Meigs et al., 2016), while others have found them to increase (Bigler et al., 2005; Halofsky et al., 2020; Wayman & Safford, 2021). Decreases in fire severity may occur because there is less live vegetation after beetle outbreak (Meigs et al., 2016), but this relationship may be complicated by other factors, such as fire weather, local fuel gradients, mixed beetle-caused mortality, and difficulties in sampling (Ager et al., 2007; Berg et al., 2006; Hicke et al., 2012; Lundquist, 2007). Based on field observation in mixed-conifer forest in California, Wayman & Safford, (2021) found fire severity increased when the level of beetle-caused mortality was below 40%, while fire severity stopped increasing at higher levels of mortality.

Because the factors influencing wildfire responses to beetle outbreaks can interact in complex ways, it is difficult to characterize mechanistic relationships among them using observational studies and/or controlled experiments, which are often constrained by data limitations and difficulty in controlling the confounding variables that occur in the field (Hicke et al., 2012). Simulation models can enable controlled experiments that help us to characterize how fuels and fire behavior vary in response to a range of outbreak severities (i.e., beetle-caused tree mortality; Ren et al., 2022) and site-specific environmental conditions during different phases of beetle outbreaks (Bond et al., 2009; Hicke et al., 2012; McCarley et al., 2017).

The overarching objective of this paper is to understand how fuels and wildfire regimes respond to beetle-caused tree mortality across a range of environmental conditions and post-outbreak time periods. Specifically, we asked the following questions:

1. How do wildfire regimes (surface fire size and probability, and surface and crown fire severity) respond to beetle outbreaks during different phases of outbreak (i.e., the red phase, gray phase, and old phase)?
2. How does the percentage of beetle-caused tree mortality influence post-outbreak wildfire regimes?
3. How do pre-outbreak fuel conditions (i.e., fuel loading and fuel aridity) affect wildfire regimes after beetle outbreaks?

2 Methods

2.1 Study area

Trail Creek is a 167-km^2 sub-catchment of the Big Wood River basin, located in Blaine County (Idaho, US) between the Salmon-Challis National Forest and Sawtooth National Forest (43.44ºN, 114.19ºW; Figure 2). Trail Creek experiences cold, wet winters and warm, dry summers. The mean annual precipitation is around 900 mm, of which 60% falls as snow (Frenzel, 1989). Trail Creek has a strong elevation gradient, ranging from 1760 to 3478 m, which also coincides with gradients in aridity and vegetation cover. Lower to middle elevations are arid and covered by sagebrush, riparian species, and grass; middle to higher elevations are relatively humid and are covered by Douglas-fir (*Pseudotsuga menziesii*), lodgepole pine (*Pinus contorta varlatifolia*), subalpine fir (*Abies lasiocarpa*), and mixed shrub and herbaceous vegetation (Buhidar, 2001). There are no records of large wildfires (> 400 hectares) occurring in Trail Creek over the last 40 years (MTBS, Eidenshink et al., 2007). According to LANDFIRE, Trail Creek has distinct fire regimes in the northern (high elevation) and the southern (low elevation) portions of the watershed. The northern part of the basin is flammability limited with an approximate 200-year FRI (Table 1; Rollins, 2009) and the southern part of the basin is fuel-limited, with a 35-year fire return interval (FRI);. Some transitional areas experience a mixed severity fire regime with 35 to 200-year FRIs. An aridity gradient, defined as the ratio of average annual potential evapotranspiration (PET) to average annual precipitation (P) over a 38-year period (1980-2018), generally overlaps with these fire regime groups (Figure 2a, Table 1).

Table 1. Fire regime groups (Rollins, 2009) and corresponding characteristics for Figure 2.

Fire Regime Group	Fire Characteristics
Fire Regime Group I	<= 35-year Fire Return Interval (FRI), low and mixed severity

Fire Regime Group III	35 to 200-year FRI, low and mixed severity
Fire Regime Group IV	> 200-year FRI, any severity

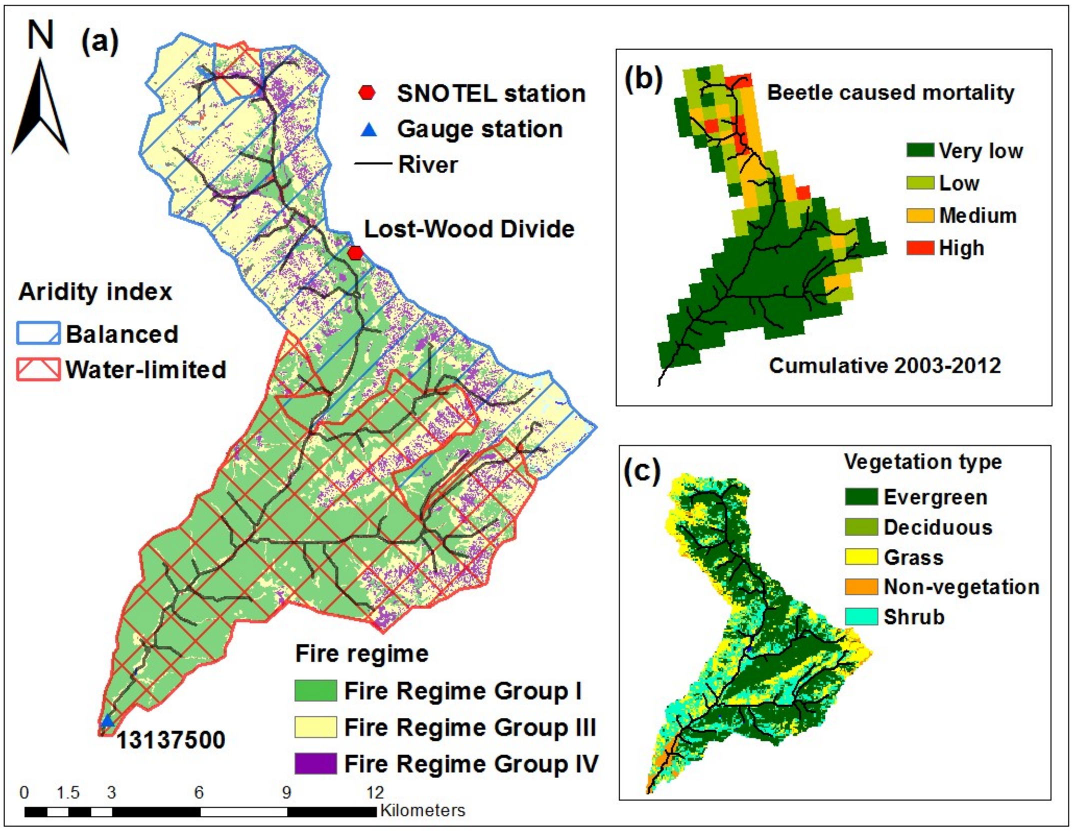

Figure 2. Study site – Trail Creek located in Idaho, US, is a sub-catchment of the Big Wood River basin. Panel (a) shows fire regimes based on LANDFIRE (Rollins, 2009). The outlined diamond grids and diagonal stripes show different zones according to an aridity index (i.e., annual mean potential evapotranspiration (PET)/precipitation (P)) calculated from historical 38-year meteorological data: PET/P>2 is water-limited, PET/P<0.8 is energy-limited, PET/P between 0.8 and 2 is balanced. Panel (b) shows beetle caused tree mortality from 2003 to 2012 (Meddens et al., 2012) overlapped with topography (elevations range from 1760 to 3478m. Panel (c) shows land cover map (Dewitz, 2019).

2.2 Model descriptions

2.2.1 Ecohydrological model

We used a coupled ecohydrologic-fire regime-beetle effects model (RHESSys-WMFire-Beetle) to understand the effect of beetle-caused mortality on fire regimes. This framework couples the Regional Hydro-ecologic Simulation System (RHESSys) with models for fire spread (WMFire; Kennedy et al., 2017), fire effects (Bart et al., 2020), and beetle effects (Ren et al., 2021). RHESSys is a distributed, process-based land surface model that simulates how climate and land use changes influence biogeochemical cycling and hydrology (Tague & Band, 2004). It has been widely tested and applied in mountainous watersheds across the Pacific Northwest, western North America, and globally (e.g., Garcia & Tague, 2015; Hanan et al., 2017, 2018, 2021; Lin et al., 2019; Ren et al., 2021; Son & Tague, 2019; Tague & Peng, 2013). A more detailed description of the RHESSys model can be found in Text S1 in the supplementary material and papers by Garcia et al., 2016; Tague & Band, 2004; Tague et al., 2013).

2.2.2 Fire spread and fire effect models

WMFire is a stochastic fire spread model coupled with RHESSys (Kennedy et al., 2017). The coupled model has previously been tested and applied in the Western US and can reproduce expected fire regimes (Hanan et al., 2021; Kennedy et al., 2017, 2021; Ren et al., 2022). It calculates the probability of fire spread (P_s) over time and space based on dead surface fuel loading (i.e., litter carbon), fuel aridity (i.e., relative deficit; 1 – evapotranspiration/PET), wind speed and direction, and topographic slope, which are outputs from RHESSys. WMFire then produces maps of P_s over randomized ignitions and stochastic spread to produce fire size distributions over time. A fire effects model connects fire spread to fire severity, which in turn modifies RHESSys litter and vegetation state variables (Bart et al., 2020). Fire effects include vegetation mortality and consumption of vegetation, litter, and coarse woody debris (CWD). Crown fire severity is simulated as a function of surface fuels and understory consumed and canopy height structure. Consequently, these simulated fire effects can influence the post fire hydrologic and biogeochemical fluxes and their interactions with vegetation and fuel recovery (Hanan et al., 2021). WMFire is a stochastic model and requires approximately 200 replicate simulations to simulate a representative fire regime (Kennedy, 2019).

2.2.4 Beetle effects model

Ren et al., (2021) also coupled a beetle effects model with RHESSys-WMFire (modified from (Edburg et al., 2011). This model includes a dead foliage pool (i.e., red needles that remain on trees) and a snag pool (i.e., standing dead tree stems) as additional carbon (C) and nitrogen (N) stores in RHESSys. After beetle-kill, leaf C and N are immediately moved from the leaf into the dead foliage pools and they remains on the canopy for one or more years, per user input (here we used 1 year; Edburg et al., 2011; Meddens et al., 2012). After a year, dead foliage C and N are transferred from the canopy to litter C and N stores using an exponential decay rate (we prescribe a half-life of two years). Similarly, stem C and N remain in the snag pool for several years (here we prescribe five years) and are then transferred into a CWD pool with an exponential decay rate (here we prescribe a half-life of ten years from snag pool to CWD). In the beetle effects model, we calculate two Leaf Area Indices (LAIs): Total LAI includes both the dead foliage and live leaves in the canopy; while Live LAI only includes the live leaves. Total LAI can affect how the canopy intercepts precipitation and radiation (Ren et al., 2021). The overstory canopy height is calculated as a function of both live stem C and snag C. In this study, we assume same beetle–caused mortality level for all evergreen patches across a landscape. Also, when fire spreads from the ground to the overstory canopy, it consumes the same fractions of snags and dead foliage as stems and live leaves.

2.3 Input data

We used US Geologic Survey National Elevation Dataset (NED, Gesch et al., 2018) to calculate slope and aspect across Trail Creek, and then delineate basin and sub-basin boundaries using the GRASS GIS tool r.watershed. We aggregated topographic data to generate patches with a resolution of 100-m. We used vegetation cover categories (including evergreen, deciduous, shrub, grass, and unvegetated; i.e., bare ground or urban) from the National Land Cover Database (NLCD 2016; Dewitz, 2019) and soil texture (i.e., sandy loam and loam) from the spatially continuous probability soils map (POLARIS, Chaney et al., 2016). In total, our model setup included 72 sub-basins and 16,705 patches, of which, 49.6% were evergreen, 24.9% were shrub, 22.1% were grass, 0.3% were deciduous, and 3.1% were not vegetated.

We acquired meteorological inputs, including maximum and minimum temperatures, precipitation, relative humidity, radiation, and wind speed, from high-resolution (1/24th degree or ~4-km) gridMET datasets for the years 1979-2017 (Abatzoglou, 2013). Then, to extend the gridMET record back for the years 1900 to 1978, we used ERA-20C daily reanalysis data (spanning 1900 – 2010), which is interpolated to match the gridMET resolution (Poli et al., 2016). The resulting daily data (1900 – 1978) was bias corrected to match the gridMET for each month based on the overlapping period for the two datasets (1979 -2010) as described per (Hanan et al., 2021). We further bias corrected the 1900 – 1978 data with PRISM (Daly et al., 1994).

2.4 Simulation experiments

To examine how beetle-caused tree mortality affects fire regimes (specifically fire size, burn probability and fire severity), we ran a series of model simulations spanning the years 1910-1990 using the coupled RHESSys-WMFire and beetle effects model. In each scenario, we prescribed different mortality levels on September 1 1915 and then simulated 75 years following the outbreak. Consequently, the simulation period captured three phases after beetle outbreak, but ends prior to significant 21st century climate change effects on fuel conditions (Hanan et al., 2022; Tang & Riley, 2020). We defined the pre-outbreak phase as the period before beetle outbreaks (1910 – 1914), the red phase as 0-5 years post-outbreak (1915 – 1920), the gray phase as 6-15 years post-outbreak (1921 – 1930), and old phase as 16-75 years post-outbreak (1931-1990).

We prescribed 9 beetle-caused mortality levels ranging from 10% to 90% C removal (in 10% increments) and applied each level uniformly to all evergreen patches (Figure 2c). We also included a no-mortality scenario as a control run, resulting in 10 total fire "on" scenarios (Table 2).

Table 2. Description of simulation scenarios. The beetle-caused mortality scenarios were for increments of 10% between 10% and 90% mortality.

	scenarios	**Beetle effects model**	**Fire spread and effects model**	**Number of simulations**
Fire scenarios	Control (no beetle outbreak)	off	on	200
	Mortality (10% - 90%)	on	on	200 for each mortality level
No-fire scenarios	Control (no beetle outbreak)	off	off	1
	Mortality (10% - 90%)	on	off	One for each mortality level

The modeled differences in fire characteristics between mortality scenarios and the control run represent the fire responses to beetle outbreaks. To better understand the fire severity responses to beetle outbreak, we also ran an additional 10 fire "off" scenarios (i.e., one for each mortality level) and examined the differences in C pool between the fire and no fire scenarios. We considered surface and crown fire severity to be the net C loss caused by fire in the litter and overstory pools, respectively.

We used mean fire size and burn probability (P_{burn}) as key metrics of fire regime responses. The mean fire size was calculated as the mean number of patches burned per fire. For each 100-m patch, the P_{burn} of surface fire was calculated as:

$$p_{burn} = \frac{number\ of\ time\ burned\ acr\quad all\ simulations}{number\ of\ simulation\ years * number\ of\ simulations} \qquad \text{Equation 1}$$

To compare our simulation results with literature, we selected a set of model outputs as surrogates for fuel and fire characteristics (Table 3). We used litter C and overstory leaf C to represent dead surface fuel and canopy fuel dynamics, respectively. For fire characteristics, we focused on the probability of surface fire occurrence (represented as P_{burn}), surface fire severity (represented as litter C lost), and crown fire severity (represented as canopy C lost). Because WMFire only simulates fire starts at the surface, we did not include the probability of crown fire occurrence in our analysis.

Table 3. Definitions of fuel and fire characteristics potentially affected by bark beetle-caused tree mortality (Modified from (Hicke et al., 2012). The model output column is the corresponding model output for different fuel and fire characteristics examined in the result section.

Category	Characteristics	Model output	Definition
Canopy fuels	Canopy fuel loads	Overstory leaf C	Mass of fuel in canopy

Dead surface fuels	Fine fuel loads	Litter C	Litter; dead surface fuels <1’’ in diameter
Fire	Probability of surface fire occurrence	Burn probability (P_{burn})	Probability that fire occurs
	Surface fire severity	Net litter C loss	Effects of fire on ecosystem properties (changes in surface fine fuel loading)
	Crown fire severity	Overstory tree canopy leaf C loss	Effects of fire on ecosystem properties (changes in canopy fuel loading)

3 Results

3.1. Basin-scale vegetation and fuel responses to beetle-caused tree mortality in the absence of fire

During the **red phase** (1915 – 1920), more than 50% of dead foliage fell to the ground and snags remained standing as prescribed by the beetle effects model (Figure 3*, e&f*). However, litter C remained lower than in the control run because beetle kill reduced plant productivity and litter accumulation, and a large portion of carbon remained locked up in the dead foliage and snag pools in the first few years after beetle outbreak. The live leaf area index (Live LAI) was smaller in the mortality than in the control (no-mortality) simulations but exhibited a faster recovery rate than the control run in the first five years after beetle outbreak (Figure 3*a*). Fuel aridity decreased compared to the control run, due to lower Live LAI in all beetle-caused mortality scenarios (low Live LAI reduced PET, thereby reducing fuel water deficit; Figure 3*c*). Unlike Live LAI, Total LAI (which includes live leaves and dead canopy foliage) increased in the red phase because beetle-caused mortality increased growth in surviving trees and understory plants, while dead foliage also remained in the canopy (Figure 3*b*).

In the **gray phase** (1921-1930), snags started falling to the ground and no dead foliage remained on the canopy (Figure 3 e&f). The dead surface fuel load (i.e., the litter) was higher in the nine beetle-caused mortality scenarios than in the control run and increased with outbreak severity (Figure 3d). Fuel aridity did not differ between the mortality scenarios and the control run because differences in live LAI were much smaller between mortality scenarios and control run (Figure 3 a&c).

In the **old phase** (1931-1990), all snags fell to the ground as coarse woody debris and vegetation slowly recovered. The modelled litter C peaked around 25 years after beetle outbreak (i.e., in 1940) due to snag fall and CWD decay (Figure 3d). At the end of the old phase, there was no more litter than in the control run and the live LAI also caught up the control run (Figure 3 *a&d*). During the last ten years of the old phase (1980-1990), fuel aridity also caught up with the control run as Live LAI recovered back to the level present in the control run (Figure 3 *a&c*).

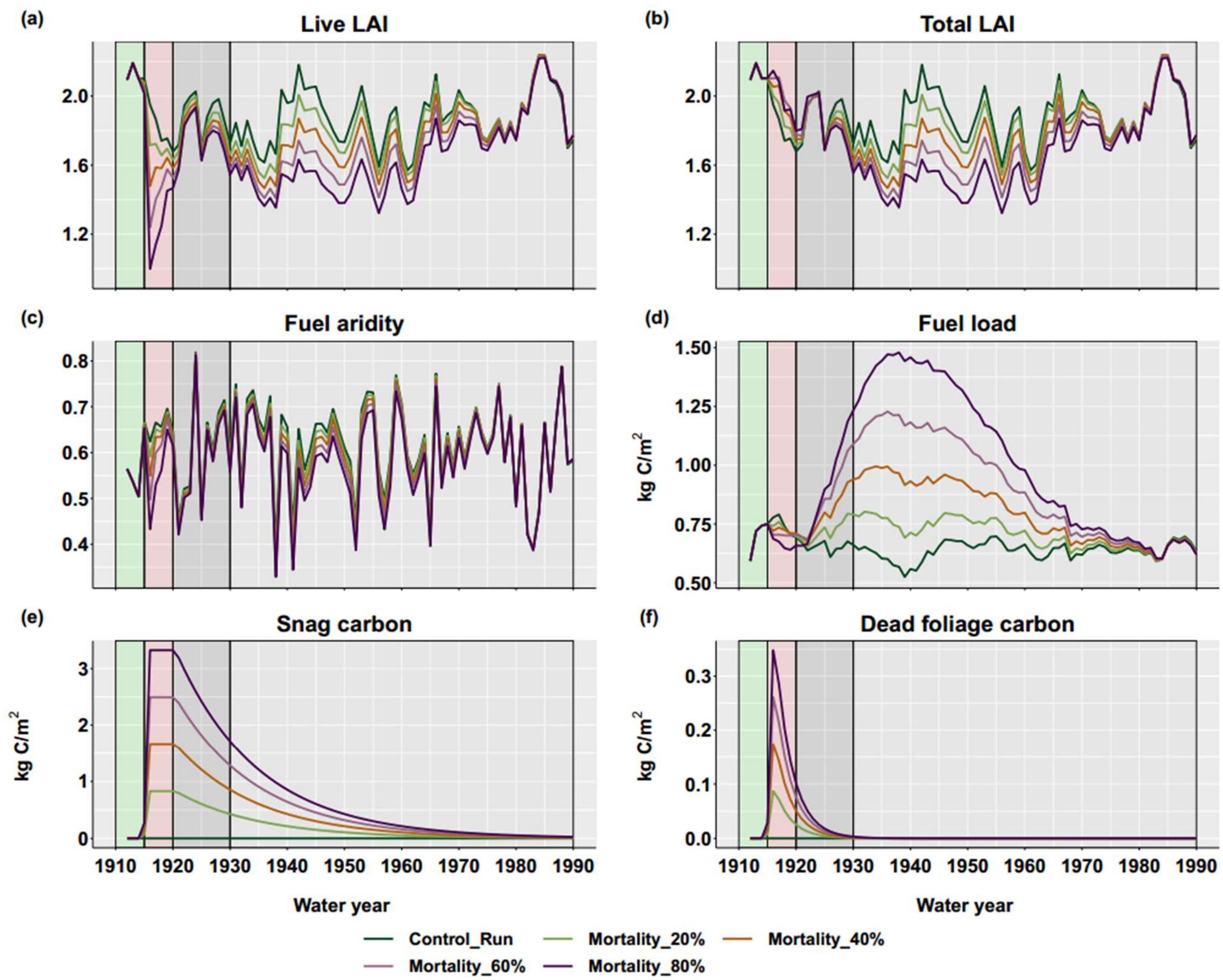

Figure 3. Basin-scale vegetation responses to beetle outbreaks. The background color corresponds to the 4 phases of beetle outbreaks: pre-outbreak (before 1915), red (1915-1920), gray (1921-1930), and old (1931-1990) phases. Fuel load is represented as litter C pool from the model, fuel aridity is calculated as 1 – ET /PET, ET is evapotranspiration.

3.2 Fire size characteristics

Fire size responded differently in each outbreak phase. In the ***red phase***, fire size decreased or did not change (Figure 4). At low beetle-caused mortality (<=20%), there were no obvious changes in the distribution of fire sizes compared to the control run. At medium to high beetle-caused mortality (>20%), fire size decreased with increasing mortality (Figure 4). This was mainly due to decreases in fuel loading caused by reduced tree productivity (Figure 3d).

In the ***gray phase***, fire size generally increased except under low mortality scenarios (<=20%) which exhibited a slight decrease (Figure 4, gray phase). Fire size increased with mortality but reached a plateau at a 50% mortality. Above 50% mortality, the median fire size remained elevated and the occurrence of large fires increased (i.e., the distribution shifted to have a longer tail towards larger fires). In a fuel-limited system, increasing fuel loading can lead to larger fires. However, once fuel loads are no longer limiting, fire size will stop responding to increasing fuel loading and will instead respond more to changes in fuel aridity (Figure S2). In higher mortality scenarios (>50%), we found that fuel aridity did not differ from the control run during the gray phase, nor did fire size (Figure 3c).

In the ***old phase***, fire size exhibited a non-monotonic response to beetle-caused mortality (Figure 4). Under low mortality (<=20%), fire size was smaller or similar to the control run. Medium mortality (>20% and <=50%) increased fire size relative to the control run, and the magnitude increased with greater mortality. Under high mortality (>50%), fire size generally decreased, and the magnitude was similar among different mortality scenarios. This variability occurred because increases in fuel loading from snag- and needle- fall and decreases in fuel aridity from reduced plant water demand had competing effects and the dominant effects differed among different levels of mortality, which will be explained in section 4.1. The P_{burn} response to mortality levels during the three phases were similar to fire size responses with some spatial variations (see Text S3 in supplementary material for details).

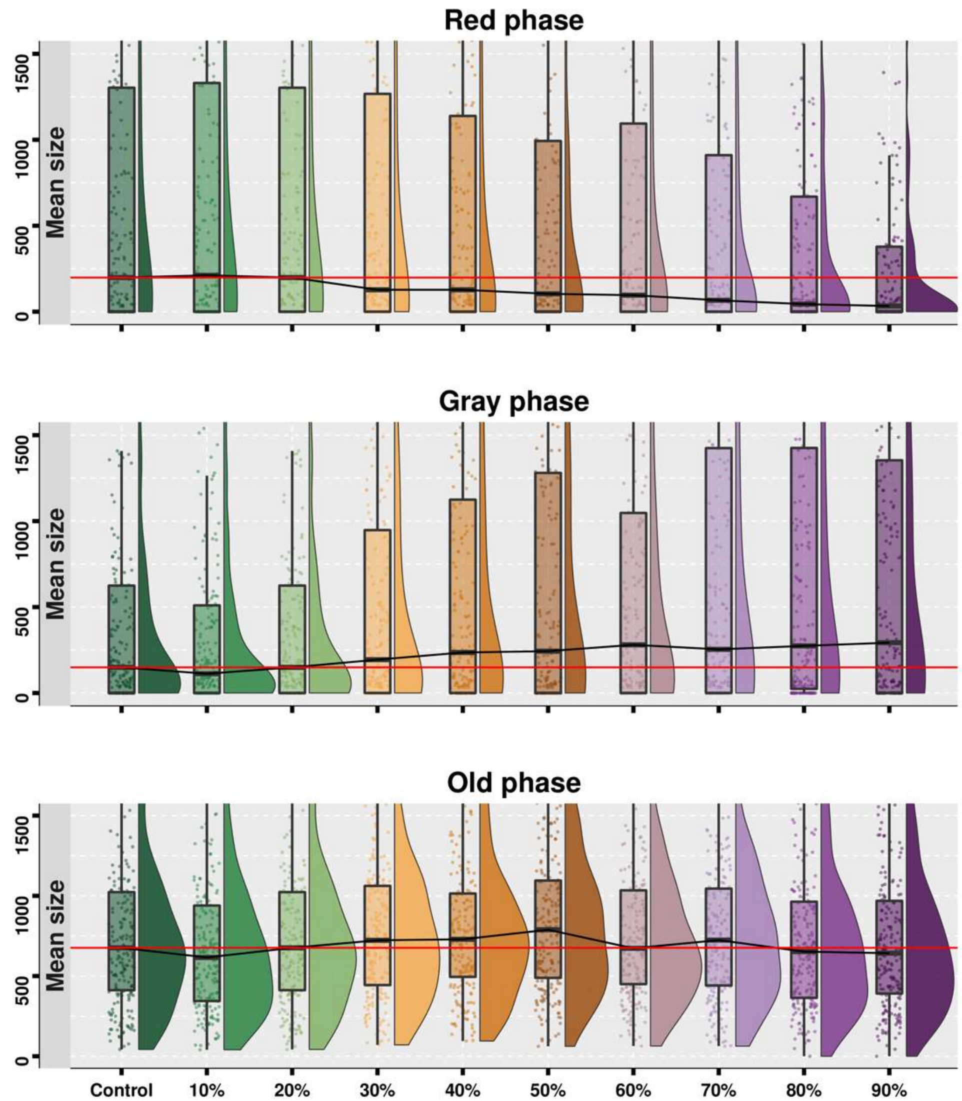

Figure 4. Distribution of mean fire sizes (number of patches burned) for each phase. Distributions come from 200 replicate simulations for each scenario. Box plots show 25th, median, 75th percentile for mean fire size, the red line is the median value for the control run, and the black line connects the median for each scenario. Low beetle-caused mortality is 10 – 20%, medium mortality is 20-50%, and high mortality is > 50%.

3.3 Fire severity

Surface fire severity responded differently during different outbreak phases (Figure 5). ***In the red phase***, for the control run (i.e., the no outbreak scenario), surface fire severity was driven by single large fire events (Figure S4, 1917 fire). Following low and medium beetle-caused mortality (<=50%), fire severity decreased slightly compared to the control (no beetle outbreak) scenario, but the decreases did not change with mortality level (Figure 5). Following high mortality (>50%) scenarios, fire severity decreased substantially in response to decreases in fuel loading (Figure 3*d*). ***In the gray phase***, during medium to high mortality (>=20%), fire severity increased with increasing mortality, especially for the second half of the gray phase (Figure S4 and Figure 5) due to increases in fuel loading that were driven by dead foliage and snagfall (Figure 3d). ***In the old phase***, with low to medium mortality (<=50%), surface fire was more severe and the severity increased with higher mortality (Figure 5; Figure S4*,* median, 95^{th} percentile, and maximum fire severity were all further away from the top green line; i.e., the no fire scenario). With high mortality (>50%), fire severity reached an upper limit and stopped increasing with higher mortality. However, in some extreme events, surface fire severity increased with increasing mortality and could sometimes even reduce surface fuel loads back to their pre-outbreak level (e.g., Figure 5 old phase and Figure S4 mortality 90% scenario).

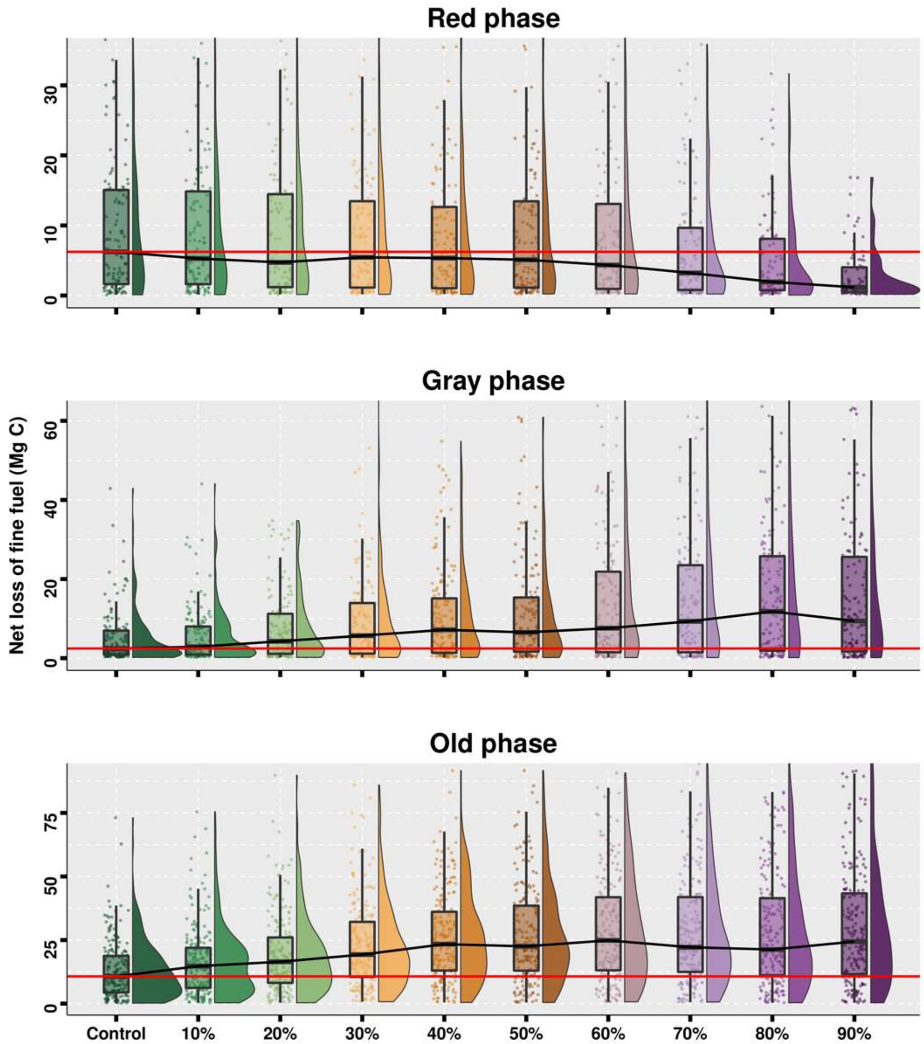

Figure 5. Distribution of surface fire severity for each phase. Distributions come from 200 simulation replicates for each scenario. Box plots show 25th, median, and 75th percentile values for fine fuel C loss. The red line is the median value for the control run, the black line connects the median line for each scenario. Low beetle-caused mortality is 10-20%; medium mortality is 10-50%; and high mortality is larger than 50%. Notice that the y-axis is different for different phases to better illustrate the extreme fire severity.

Overstory leaf C (both live leaf and dead foliage) loss caused by fire can be a metric of crown fire severity. In general, crown fire responded similarly to beetle-caused mortality as did surface fires (Figure 6 and Figure S5). However, the timing of severe crown fires exhibited some unique patterns (Figure 6). First, the increases in crown fire severity were more evident after around 25 years post-outbreak (i.e., after 1940; Figure 6A, illustrated by the difference between the dashed line and solid lines). This is around the time when fuel loading peaked, and canopy height was low (Figure 3*d* and Figure S6). This occurred because snagfall and increasing litter loads enabled fire to spread to the overstory more easily. Second, in high mortality scenarios, extreme fire events consumed 60% to 70% of canopy C, which is characteristic of a high severity/stand replacing fire regime (Figure 6B, illustrated by the decrease in the distance of the lighter orange band from the top). In high mortality scenarios, fire can be more severe even if it is less frequent (Figure S3).

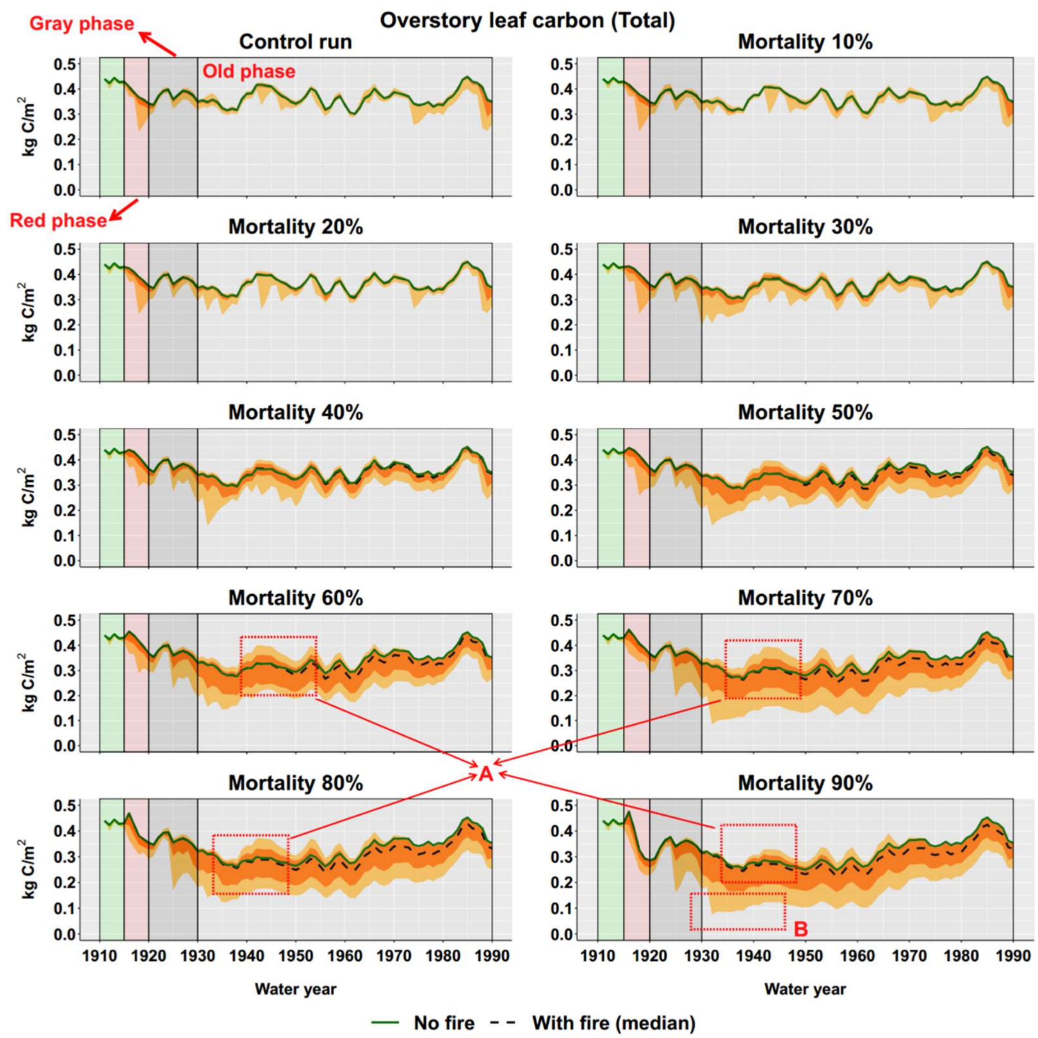

Figure 6. Distribution of leaf C for the 200 fire simulations and the no fire scenario (all means include both live leaf and dead foliage killed by beetle outbreaks. The dashed line is the median

litter state for the fire scenarios; and the solid green line is the no fire scenario. Light orange shading shows the maximum and minimum litter C, dark orange shows the 5th and 95th percentile litter C. The differences between the no-fire scenario (green line) and fire scenarios (other lines) can be a surrogate for cumulative fire severity. See Figure S9 for detailed surface fire severity results.

4 Discussion

Understanding and managing fire risk in landscapes that are vulnerable to bark beetle outbreaks requires examining how fuel conditions changes over space and time. We examined how the extent of mortality, pre-outbreak fuel conditions, and time since outbreak can influence fire regimes using a novel ecohydrologic-fire regime-beetle effects model (RHESSys-WMFire-Beetle) in a semiarid watershed in the western US. We found that fire size and probability decreased in the red phase, increased in the gray phase, and had mixed responses in the old phase contingent on the level of beetle-caused tree mortality. The influence of time after outbreak on fire was a function of changes in fuel loading and fuel aridity that emerged from vegetation growth dynamics, snagfall, and litterfall from dead foliage. There was a complex non-linear relationship between the extent of mortality and fire responses. There were also no significant differences in surface fire probability following low mortality (<=20%), and fire probability leveled off or started decreasing following high mortality (>50%).

4.1 Effects of pre-outbreak fuel conditions on wildfire responses

Fuel loading and fuel aridity can compound or counteract one another to drive fire regimes. In locations that were fuel-limited prior to outbreak, fire probability increased in response to increasing fuel loading from beetle-caused tree mortality (Figure 7*a*). However, areas that were less fuel-limited, increases in fuel loading and decreases in fuel aridity had opposite effects on P_{burn} and whether there was a net increase or decrease depended on the phase of outbreak. For example, once there was enough fuel from snagfall in the old phase, P_{burn} only responded to changes in fuel aridity, and fire regimes shifted from fuel-limited to flammability-limited. However, fuel aridity changes were relatively small and slow compares to changes in fuel loading (Figure 7*b*). Similarly, Kaufmann et al., (2008) found changes in fuel aridity after beetle outbreaks play an important role in driving fire hazard. Beetle-caused mortality can increase fuel loading in semiarid systems, thus shifting fire regimes from fuel-limited to flammability-limited (e.g., in the old phase).

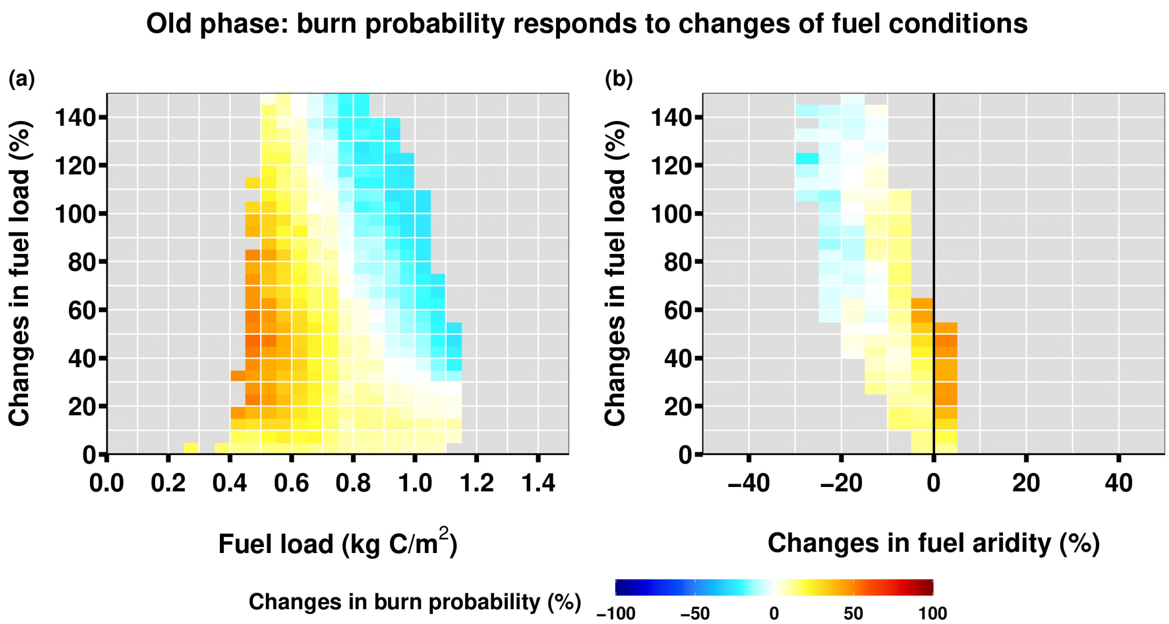

Figure 7. The response of burn probability to fuel load and its relative change and the relative change in fuel aridity during the old phase in the evergreen forest-dominated area (the changes are calculated as outbreak scenario minus control scenario). We merged all beetle outbreak scenarios together and bin the data at every 5% or 0.05 kg C/m^2. Bins with less than 100 samples are removed. The change in burn probability of each bin is the median value. The black line divides the fuel aridity into "increases" and "decreases" zone, respectively.

4.2 The effects of tree mortality level on fire responses

The extent of beetle-caused mortality played an important role in post-outbreak fire responses, although mortality effects varied among phases. Mortality level affects fuel loading and fuel aridity by altering vegetation productivity and turnover, increasing dead fuels, and transforming canopy structure. We found that surface fire probability and severity only responded to beetle outbreaks when mortality was higher than 20% and stopped increasing at around 50%. Similarly, based on field observations in mixed-conifer forests in the Sierra Nevada, Wayman and Safford (2021) reported that fire severity increased most substantially when beetle-caused mortality surpassed 15% and was below 30-40%. In this study, fire severity may have stopped increasing with mortality above 50% because plant water demand decreased, leading to decreases in fuel aridity. Although we also found an upper limit (~50%) where median fire probability and fire severity no longer increased with increasing mortality, the occurrence of extremely severe fires may continue to increase in some cases (e.g., Figure S4*,* old phase). These findings highlight the utility of modeling studies that can capture full range of possible fire responses (including extreme fires) to beetle outbreaks, while field studies are limited by the number of observations.

We also found that fire size and fire probability responses to beetle-caused mortality also varied in each post outbreak phase. There was a negative relationship between them in the red phase (i.e., higher mortality reduced fire size and probability), a positive relationship with a plateau in the gray phase, but mixed responses in the old phase. The negative relationships in both the red phase and the old phase occurred for different reasons. In the red phase, decreases in fire probability that occurred with increasing mortality were caused by reductions in fuel loading. In the old phase, when mortality was above 50%, fire probability decreased with increasing mortality in locations that were not limited by fuel loading but by fuel aridity. Like the mechanisms driving decreases in fire severity, this occurred because increasing mortality in these locations decreased fuel aridity. Such mechanisms may also explain decreases in fire activity observed in other flammability-limited landscapes (e.g., Bebi et al., 2003; Kulakowski et al., 2003).

Fuel aridity changes in high mortality scenarios were important factors driving different impacts of beetle outbreak on fire probability and fire severity. For example, fire severity and fire probability responses were similar in the red phase, but different in the gray and old phases (Figure 8). In the gray phase, surface fire severity increased with greater mortality even after fire probability plateaued (Figure 8). This occurred because enough fuel was still available to burn once fire spread to a given location. In the old phase, surface fire probability decreased following high mortality but fire severity remained elevated. We also found that for some extreme fire events, surface fire severity still increased with increasing mortality even when fire probability decreased (Figure S3 & Figure S4). High mortality increased fuel moisture, which may have limited the probability of fire, but once weather conditions were suitable for fire to spread, increased fuel loads led to higher fuel consumption. These tradeoffs may explain some of the contradictory findings in recent field observations. When mortality is moderate, its effects on fuel moisture do not dominate over increases in fuel loading—thus increasing fire severity (Harvey et al., 2014; Metz et al., 2011; Prichard & Kennedy, 2014). However, when mortality is high, reductions in fuel aridity can reduce fire probability, leading to decreases in fire occurrence, even though there is more fuel available to burn and under the right circumstances, the likelihood of a severe fire may increase (Andrus et al., 2016; Kulakowski et al., 2003; Meigs et al., 2016).

4.3 The effects beetle outbreak phases on fire responses

The effects of beetle outbreaks on fire probability and severity vary among the red, gray, and old phases following attack. In the conceptual framework developed by Hicke et al., (2012;

Figure 1), surface fire probability does not change in the red phase and increases in the gray and old phases due to increases surface fuel loading. Additionally, crown fire severity is hypothesized to increase in the red phase but decrease in the gray and old phases due to changes in canopy fuel loading and leaf moisture. Here we refine and expand this conceptual framework using results from our process-based modeling study (Figure 8 and Table S1).

We found that in our semiarid watershed, during the **red phase**, surface fire probability and severity had opposite responses than those hypothesized by Hicke et al., (2012). For example, their framework suggests that beetle outbreaks do not increase surface fire probability or fire severity during the red phase because they do not substantially change dead surface fuel loading (Figure 1; Bebi et al., 2003; Berg et al., 2006; Bond et al., 2009; Hicke et al., 2012). However, we found that modeled surface fire probability and severity decreased during the red phase because beetle outbreaks reduced vegetation productivity and dead foliage initially lingered in the canopy, leading to an initial decrease in surface fuels. Our results are corroborated by field studies that have found fire severity can decrease during the red phase in the U.S. Pacific Northwest, due to decreases in live vegetation (Meigs et al., 2016).

Our modeling study further extends the Hicke et al., (2012) conceptual framework by accounting for the effects of surviving vegetation on fuel accumulation during the red phase. However, these modeling results only reflect one possible outcome because surface fuel loading responds to both vegetation productivity and the rate of litterfall. In our model, litterfall from dead foliage is controlled by two parameters: *delay time* and *rate of dead foliage fall*. If the delay time is shorter and dead foliage fall is faster than typical leaf phenology in the no outbreak scenario, litter loading may increase, thereby increasing fire probability. Furthermore, the relatively short length of the red phase (<= 5 years) and the fact that beetles can attack trees for multiple years (leading to a mixture of phases in a given location) increases the uncertainty surrounding fire responses (Jolly, Parsons, Varner, et al., 2012).

In the **old phase**, changes in surface fuel aridity are an important factor causing discrepancies between our model study and the conceptual framework. Although we found that surface fire probability increased when mortality was lower than 50%, it decreased when mortality was higher. The differences at high mortality may have occurred because the (Hicke et al., 2012) conceptual framework only considered the effects of increases in surface fuel loading and did not consider the possible effects of decreases in fuel aridity. We found that in high mortality scenarios, fire probability decreased because decreases in fuel aridity dominated over increases in fuel loading. Similarly, Kulakowski et al., (2003) reconstructed historical disturbance data in Colorado and concluded that surface fire probability can decrease after beetle outbreaks due to increases in fuel moisture.

We found that the largest differences between our model and the Hicke et al., (2012) conceptual model occurred with crown fire severity. Crown fire severity is driven in large part by changes in leaf moisture and surface fire probability, which can counteract one another. In their conceptual framework, Hicke et al., (2012) suggested that in the red phase, crown fire severity increases due to decreases in leaf moisture (Figure 1). However, our model did not account for how changes in dead leaf moisture influence fire propagation to the canopy. Instead, we found that crown fire severity decreased due to decreases in surface fire probability (Figure 8).

In the old and gray phases, Hicke et al., (2012) suggested that decreases in crown fire severity occurred because decreases in canopy fuel dominated over increases in ground fire probability. However, we found the opposite to be true—increases in ground fire probability and lower overstory canopy dominated over decreases in canopy fuel, leading to a net increase in canopy fire severity. Similarly, Turner et al., (1999) found crown fire severity could increase when the connection between ground and canopy fuels increased. Thus, the conceptual framework should be expanded to consider canopy fuel structure when predicting crown fire responses to beetle outbreaks.

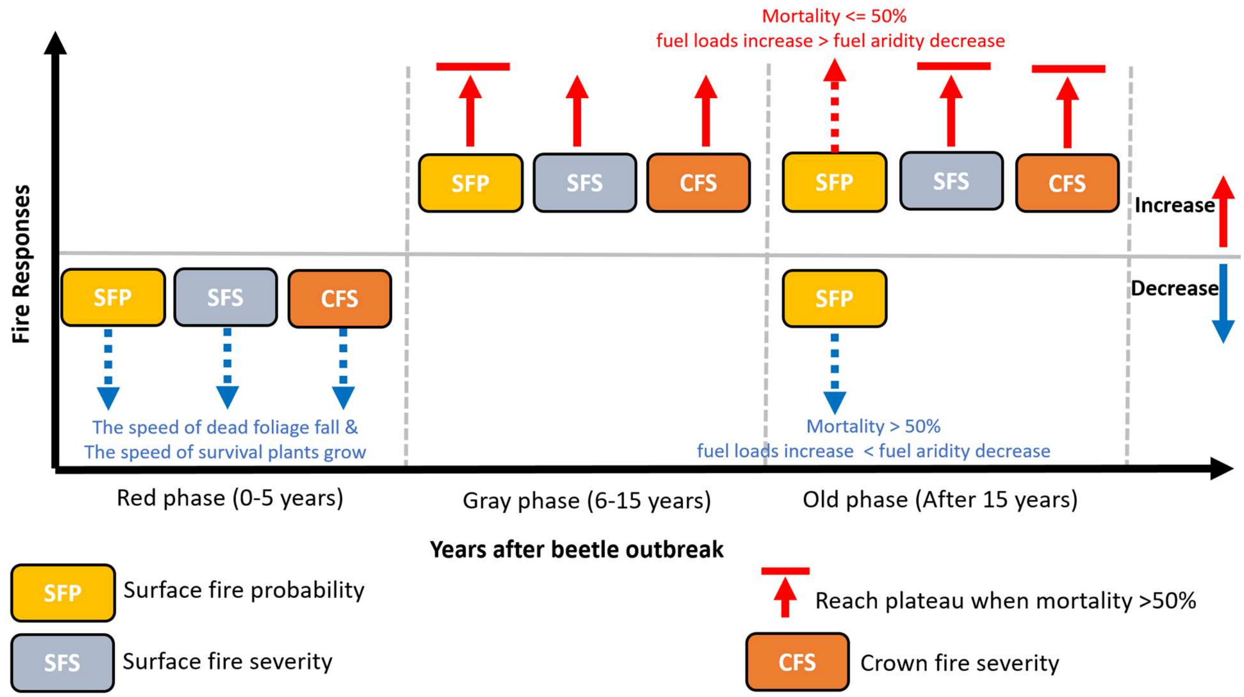

Figure 8. Revised conceptual model showing fire responses to beetle outbreaks from our research. A summary of detailed mechanisms is described in . The dashed arrow means the fire responses is uncertain and depend on the dominate mechanisms. In red phase, fire responses depend on the speed of dead foliage fall and survival plants grow. In old phase, surface fire probability changes depend on the competition between increase in fuel loading and decrease in fuel aridity after beetle outbreaks. When mortality is smaller than 50%, increase in fuel loading dominates over decrease in fuel aridity cause an increase in surface fire probability, and vice versa for mortality larger than 50%.

5. Conclusion

Our research shows that the impacts of beetle outbreaks on fire probability and fire severity are conditioned by mortality level, phase, and pre-outbreak fuel conditions. To our knowledge, this is the first time fire regimes have been linked with beetle effects through a modeling approach that can account for the coupling among fire regimes, vegetation and litter variables and how these evolve over time following beetle outbreak. Our results also highlight the importance of how fuel loading and fuel aridity vary within watersheds. In fuel-abundant locations, fire probability may decrease following an outbreak, while in fuel-limited locations, fire probability can increase post-outbreak with increases in fuel loading (e.g., old phase). The complex interactions among mortality, local conditions, and time since an outbreak make the prediction of fire response difficult. Our novel coupled modeling framework can be applied to different watersheds to help project fire hazard following beetle outbreaks. This can support long-term management that aims to increase forest resilience and decrease vulnerability to fire.

Acknowledgement

This project is supported by National Science Foundation of United States under award numbers DMS-1520873 and DEB-1916658. Tung Nguyen and William Burke have helped to set up the RHESSys model. We also thank Nicholas Engdahl and Jan Boll for providing valuable suggestions on the manuscript.

Conflict of Interest

The authors declare no conflicts of interest relevant to this study.

Data Availability Statement

The data sets used to run simulations for this study can be found in the Open Science Forum: https://doi.org/10.17605/OSF.IO/HWMXP, and the model code can be found on github: https://doi.org/10.5281/zenodo.5156688.

References

Abatzoglou, J. T. (2013). Development of gridded surface meteorological data for ecological applications and modelling. *International Journal of Climatology*, *33*(1), 121–131. https://doi.org/10.1002/joc.3413

Ager, A. A., McMahan, A., Hayes, J. L., & Smith, E. L. (2007). Modeling the effects of thinning on bark beetle impacts and wildfire potential in the Blue Mountains of eastern Oregon. *Landscape and Urban Planning*, *80*(3), 301–311. https://doi.org/10.1016/j.landurbplan.2006.10.010

Andrus, R. A., Veblen, T. T., Harvey, B. J., & Hart, S. J. (2016). Fire severity unaffected by spruce beetle outbreak in spruce-fir forests in southwestern Colorado. *Ecological Applications: A Publication of the Ecological Society of America*, *26*(3), 700–711. https://doi.org/10.1890/15-1121

Bart, R. R., Kennedy, M. C., Tague, C. L., & McKenzie, D. (2020). Integrating fire effects on vegetation carbon cycling within an ecohydrologic model. *Ecological Modelling*, *416*, 108880. https://doi.org/10.1016/j.ecolmodel.2019.108880

Bebi, P., Kulakowski, D., & Veblen, T. T. (2003). Interactions Between Fire and Spruce Beetles in a Subalpine Rocky Mountain Forest Landscape. *Ecology*, *84*(2), 362–371. https://doi.org/10.1890/0012-9658(2003)084[0362:IBFASB]2.0.CO;2

Bennett, K. E., Bohn, T. J., Solander, K., McDowell, N. G., Xu, C., Vivoni, E., & Middleton, R. S. (2018). Climate-driven disturbances in the San Juan River sub-basin of the Colorado River. *Hydrology and Earth System Sciences*, *22*(1), 709–725. https://doi.org/10.5194/hess-22-709-2018

Berg, E. E., David Henry, J., Fastie, C. L., De Volder, A. D., & Matsuoka, S. M. (2006). Spruce beetle outbreaks on the Kenai Peninsula, Alaska, and Kluane National Park and Reserve, Yukon Territory: Relationship to summer temperatures and regional differences in disturbance regimes. *Forest Ecology and Management*, *227*(3), 219–232. https://doi.org/10.1016/j.foreco.2006.02.038

Bigler, C., Kulakowski, D., & Veblen, T. T. (2005). Multiple Disturbance Interactions and Drought Influence Fire Severity in Rocky Mountain Subalpine Forests. *Ecology*, *86*(11), 3018–3029. https://doi.org/10.1890/05-0011

Bond, L. M., Lee, E. D., Bradley, M. C., & Hanson, T. C. (2009). Influence of Pre-Fire Tree Mortality on Fire Severity in Conifer Forests of the San Bernardino Mountains, California. *The Open Forest Science Journal*, *2*(1), 41–47. https://doi.org/10.2174/1874398600902010041

Buhidar, B. B. (2001). The Big Wood River Watershed Management Plan. *Idaho Department of Environmental Quality, Twin Falls Regional Office, Twin Falls, ID*.

Chaney, N. W., Wood, E. F., McBratney, A. B., Hempel, J. W., Nauman, T. W., Brungard, C. W., & Odgers, N. P. (2016). POLARIS: A 30-meter probabilistic soil series map of the contiguous United States. *Geoderma*, *274*, 54–67. https://doi.org/10.1016/j.geoderma.2016.03.025

Daly, C., Neilson, R. P., & Phillips, D. L. (1994). A Statistical-Topographic Model for Mapping Climatological Precipitation over Mountainous Terrain. *Journal of Applied Meteorology*, *33*(2), 140–158. https://doi.org/10.1175/1520-0450(1994)033<0140:ASTMFM>2.0.CO;2

Dewitz, J. (2019). National Land Cover Database (NLCD) 2016 Products. U.S. Geological Survey data release. Retrieved from https://doi.org/10.5066/P96HHBIE

Edburg, S. L., Hicke, J. A., Lawrence, D. M., & Thornton, P. E. (2011). Simulating coupled carbon and nitrogen dynamics following mountain pine beetle outbreaks in the western United States. *Journal of Geophysical Research: Biogeosciences*, *116*(G4), G04033. https://doi.org/10.1029/2011JG001786

Eidenshink, J. C., Schwind, B., Brewer, K., Zhu, Z.-L., Quayle, B., & Howard, S. M. (2007). A project for monitoring trends in burn severity. *Fire Ecology*. https://doi.org/10.4996/fireecology.0301003

Frenzel, S. A. (1989). *Water resources of the upper Big Wood River basin, Idaho*. US Geological Survey.

Garcia, E. S., & Tague, C. L. (2015). Subsurface storage capacity influences climate–evapotranspiration interactions in three western United States catchments. *Hydrology and Earth System Sciences*, *19*(12), 4845–4858. https://doi.org/10.5194/hess-19-4845-2015

Garcia, Elizabeth S., Tague, C. L., & Choate, J. S. (2016). Uncertainty in carbon allocation strategy and ecophysiological parameterization influences on carbon and streamflow estimates for two western US forested watersheds. *Ecological Modelling*, *342*, 19–33. https://doi.org/10.1016/j.ecolmodel.2016.09.021

Gesch, D. B., Evans, G. A., Oimoen, M. J., & Arundel, S. (2018). The National Elevation Dataset (pp. 83–110). American Society for Photogrammetry and Remote Sensing. Retrieved from http://pubs.er.usgs.gov/publication/70201572

Goeking, S. A., & Tarboton, D. G. (2020). Forests and Water Yield: A Synthesis of Disturbance Effects on Streamflow and Snowpack in Western Coniferous Forests. *Journal of Forestry*, *118*(2), 172–192. https://doi.org/10.1093/jofore/fvz069

Halofsky, J. E., Peterson, D. L., & Harvey, B. J. (2020). Changing wildfire, changing forests: the effects of climate change on fire regimes and vegetation in the Pacific Northwest, USA. *Fire Ecology*, *16*(1), 4. https://doi.org/10.1186/s42408-019-0062-8

Hanan, E. J., Tague, C. (Naomi), & Schimel, J. P. (2017). Nitrogen cycling and export in California chaparral: the role of climate in shaping ecosystem responses to fire. *Ecological Monographs*, *87*(1), 76–90. https://doi.org/10.1002/ecm.1234

Hanan, E. J., Tague, C., Choate, J., Liu, M., Kolden, C., & Adam, J. (2018). Accounting for disturbance history in models: using remote sensing to constrain carbon and nitrogen pool spin-up. *Ecological Applications: A Publication of the Ecological Society of America*, *28*(5), 1197–1214. https://doi.org/10.1002/eap.1718

Hanan, E. J., Ren, J., Tague, C. L., Kolden, C. A., Abatzoglou, J. T., Bart, R. R., et al. (2021). How climate change and fire exclusion drive wildfire regimes at actionable scales. *Environmental Research Letters*, *16*(2), 024051. https://doi.org/10.1088/1748-9326/abd78e

Hanan, E. J., Kennedy, M. C., Ren, J., Johnson, M. C., & Smith, A. M. (2022). Missing climate feedbacks in fire models: limitations and uncertainties in fuel loadings and the role of decomposition in fine fuel accumulation. *Journal of Advances in Modeling Earth Systems*, *n/a*(n/a), e2021MS002818. https://doi.org/10.1029/2021MS002818

Harvey, B. J., Donato, D. C., Romme, W. H., & Turner, M. G. (2014). Fire severity and tree regeneration following bark beetle outbreaks: the role of outbreak stage and burning conditions. *Ecological Applications*, *24*(7), 1608–1625. https://doi.org/10.1890/13-1851.1

Hicke, J. A., Johnson, M. C., Hayes, J. L., & Preisler, H. K. (2012). Effects of bark beetle-caused tree mortality on wildfire. *Forest Ecology and Management*, *271*, 81–90. https://doi.org/10.1016/j.foreco.2012.02.005

Hicke, J. A., Meddens, A. J. H., & Kolden, C. A. (2016). Recent Tree Mortality in the Western United States from Bark Beetles and Forest Fires. *Forest Science*, *62*(2), 141–153. https://doi.org/10.5849/forsci.15-086

Jolly, W. M., Parsons, R., Varner, J. M., Butler, B. W., Ryan, K. C., & Gucker, C. L. (2012). Do mountain pine beetle outbreaks change the probability of active crown fire in lodgepole pine forests? *Ecology. 93(4): 941-946.*, 941–946.

Jolly, W. M., Parsons, R. A., Hadlow, A. M., Cohn, G. M., McAllister, S. S., Popp, J. B., et al. (2012). Relationships between moisture, chemistry, and ignition of Pinus contorta needles during the early stages of mountain pine beetle attack. *Forest Ecology and Management*, *269*, 52–59. https://doi.org/10.1016/j.foreco.2011.12.022

Kaufmann, M. R., Aplet, G. H., Babler, M. G., Baker, W. L., Bentz, B., Harrington, M., et al. (2008). The status of our scientific understanding of lodgepole pine and mountain pine beetles - a focus on forest ecology and fire behavior. *GFI Technical Report 2008-2. Arlington, VA: The Nature Conservancy. 13 p.* Retrieved from https://www.fs.usda.gov/treesearch/pubs/40895

Kennedy, M. C. (2019). Experimental design principles to choose the number of Monte Carlo replicates for stochastic ecological models. *Ecological Modelling*, *394*, 11–17. https://doi.org/10.1016/j.ecolmodel.2018.12.022

Kennedy, M. C., McKenzie, D., Tague, C., & Dugger, A. L. (2017). Balancing uncertainty and complexity to incorporate fire spread in an eco-hydrological model. *International Journal of Wildland Fire*, *26*(8), 706. https://doi.org/10.1071/WF16169

Kennedy, M. C., Bart, R. R., Tague, C. L., & Choate, J. S. (2021). Does hot and dry equal more wildfire? Contrasting short- and long-term climate effects on fire in the Sierra Nevada, CA. *Ecosphere*, *12*(7), e03657. https://doi.org/10.1002/ecs2.3657

Kulakowski, D., Veblen, T. T., & Bebi, P. (2003). Effects of fire and spruce beetle outbreak legacies on the disturbance regime of a subalpine forest in Colorado. *Journal of Biogeography*, *30*(9), 1445–1456. https://doi.org/10.1046/j.1365-2699.2003.00912.x

Lin, L., Band, L. E., Vose, J. M., Hwang, T., Miniat, C. F., & Bolstad, P. V. (2019). Ecosystem processes at the watershed scale: Influence of flowpath patterns of canopy ecophysiology on emergent catchment water and carbon cycling. *Ecohydrology*, *0*(0), e2093. https://doi.org/10.1002/eco.2093

Littell, J. S., McKenzie, D., Peterson, D. L., & Westerling, A. L. (2009). Climate and wildfire area burned in western U.S. ecoprovinces, 1916–2003. *Ecological Applications*, *19*(4), 1003–1021. https://doi.org/10.1890/07-1183.1

Lundquist, J. E. (2007). The Relative Influence of Diseases and Other Small-Scale Disturbances on Fuel Loading in the Black Hills. *Plant Disease*, *91*(2), 147–152. https://doi.org/10.1094/PDIS-91-2-0147

Lynch, H. J., Renkin, R. A., Crabtree, R. L., & Moorcroft, P. R. (2006). The Influence of Previous Mountain Pine Beetle (Dendroctonus ponderosae) Activity on the 1988 Yellowstone Fires. *Ecosystems*, *9*(8), 1318–1327. https://doi.org/10.1007/s10021-006-0173-3

McCarley, T. R., Kolden, C. A., Vaillant, N. M., Hudak, A. T., Smith, A. M. S., & Kreitler, J. (2017). Landscape-scale quantification of fire-induced change in canopy cover following mountain pine beetle outbreak and timber harvest. *Forest Ecology and Management*, *391*, 164–175. https://doi.org/10.1016/j.foreco.2017.02.015

Meddens, A., A Hicke, J., & A Ferguson, C. (2012). Spatiotemporal patterns of observed bark beetle-caused tree mortality in British Columbia and the western United States. *Ecological Applications : A Publication of the Ecological Society of America*, *22*, 1876–91. https://doi.org/10.2307/41723101

Meigs, G. W., Zald, H. S. J., Campbell, J. L., Keeton, W. S., & Kennedy, R. E. (2016). Do insect outbreaks reduce the severity of subsequent forest fires? *Environmental Research Letters*, *11*(4), 045008. https://doi.org/10.1088/1748-9326/11/4/045008

Metz, M. R., Frangioso, K. M., Meentemeyer, R. K., & Rizzo, D. M. (2011). Interacting disturbances: wildfire severity affected by stage of forest disease invasion. *Ecological Applications*, *21*(2), 313–320. https://doi.org/10.1890/10-0419.1

Mitchell, R. G., & Preisler, H. K. (1998). Fall Rate of Lodgepole Pine Killed by the Mountain Pine Beetle in Central Oregon. *Western Journal of Applied Forestry*, *13*(1), 23–26.

Poli, P., Hersbach, H., Dee, D. P., Berrisford, P., Simmons, A. J., Vitart, F., et al. (2016). ERA-20C: An Atmospheric Reanalysis of the Twentieth Century. *Journal of Climate*, *29*(11), 4083–4097. https://doi.org/10.1175/JCLI-D-15-0556.1

Prichard, S. J., & Kennedy, M. C. (2014). Fuel treatments and landform modify landscape patterns of burn severity in an extreme fire event. *Ecological Applications*, *24*(3), 571–590. https://doi.org/10.1890/13-0343.1

Raffa, K. F., Aukema, B. H., Bentz, B. J., Carroll, A. L., Hicke, J. A., Turner, M. G., & Romme, W. H. (2008). Cross-scale Drivers of Natural Disturbances Prone to Anthropogenic Amplification: The Dynamics of Bark Beetle Eruptions. *BioScience*, *58*(6), 501–517. https://doi.org/10.1641/B580607

Ren, J., Adam, J. C., Hicke, J. A., Hanan, E. J., Tague, C. L., Liu, M., et al. (2021). How does water yield respond to mountain pine beetle infestation in a semiarid forest? *Hydrology and Earth System Sciences*, *25*(9), 4681–4699. https://doi.org/10.5194/hess-25-4681-2021

Ren, J., Hanan, E. J., Abatzoglou, J. T., Kolden, C. A., Tague, C. (Naomi) L., Kennedy, M. C., et al. (2022). Projecting Future Fire Regimes in a Semiarid Watershed of the Inland Northwestern United States: Interactions Among Climate Change, Vegetation Productivity, and Fuel Dynamics. *Earth's Future*, *10*(3), e2021EF002518. https://doi.org/10.1029/2021EF002518

Rollins, M. G. (2009). LANDFIRE: a nationally consistent vegetation, wildland fire, and fuel assessment. *International Journal of Wildland Fire*, *18*(3), 235–249. https://doi.org/10.1071/WF08088

Seidl, R., Honkaniemi, J., Aakala, T., Aleinikov, A., Angelstam, P., Bouchard, M., et al. (2020). Globally consistent climate sensitivity of natural disturbances across boreal and temperate forest ecosystems. *Ecography*, *43*(7), 967–978. https://doi.org/10.1111/ecog.04995

Son, K., & Tague, C. (2019). Hydrologic responses to climate warming for a snow-dominated watershed and a transient snow watershed in the California Sierra. *Ecohydrology*, *12*(1), e2053. https://doi.org/10.1002/eco.2053

Tague, C., & Peng, H. (2013). The sensitivity of forest water use to the timing of precipitation and snowmelt recharge in the California Sierra: Implications for a warming climate. *Journal of Geophysical Research: Biogeosciences*, *118*(2), 875–887. https://doi.org/10.1002/jgrg.20073

Tague, C. L., & Band, L. E. (2004). RHESSys: Regional Hydro-Ecologic Simulation System—An Object-Oriented Approach to Spatially Distributed Modeling of Carbon, Water, and Nutrient Cycling. *Earth Interactions*, *8*(19), 1–42. https://doi.org/10.1175/1087-3562(2004)8<1:RRHSSO>2.0.CO;2

Tague, Christina L., McDowell, N. G., & Allen, C. D. (2013). An Integrated Model of Environmental Effects on Growth, Carbohydrate Balance, and Mortality of Pinus ponderosa Forests in the Southern Rocky Mountains. *PLOS ONE*, *8*(11), e80286. https://doi.org/10.1371/journal.pone.0080286

Tang, J., & Riley, W. J. (2020). Linear two-pool models are insufficient to infer soil organic matter decomposition temperature sensitivity from incubations. *Biogeochemistry*, *149*(3), 251–261. https://doi.org/10.1007/s10533-020-00678-3

Turner, M. G., Romme, W. H., & Gardner, R. H. (1999). Prefire heterogeneity, fire severity, and early postfire plant reestablishment in subalpine forests of Yellowstone National Park, Wyoming. *International Journal of Wildland Fire*, *9*(1), 21–36. https://doi.org/10.1071/wf99003

Wayman, R. B., & Safford, H. D. (2021). Recent bark beetle outbreaks influence wildfire severity in mixed-conifer forests of the Sierra Nevada, California, USA. *Ecological Applications*, *31*(3). https://doi.org/10.1002/eap.2287

[Journal of Advances in Modeling Earth Systems]

Supporting Information for

Bark Beetle Effects on Fire Regimes Depend on Underlying Fuel Modifications in Semiarid Systems

[1,2]Jianning Ren, [2]Erin J. Hanan, [3]Jeffrey A. Hicke, [4]Crystal A. Kolden, [4]John T. Abatzoglou, [5]Christina (Naomi) L. Tague, [6]Ryan R. Bart, [7]Maureen C. Kennedy, [1]Mingliang Liu, [1]Jennifer C. Adam

[1] Department of Civil & Environmental Engineering, Washington State University, 99164, Pullman, USA

[2] Department of Natural Resources and Environmental Science, University of Nevada, Reno, 89501, Reno, USA

[3] Department of Geography, University of Idaho, 83844, Moscow, USA

[4] Management of Complex Systems, University of California, Merced, 95343, Merced, USA

[5] Bren School of Environmental Science & Management, University of California, Santa Barbara, 93106, Santa Barbara, USA

[6] Sierra Nevada Research Institute, University of California, Merced, 95343, Merced, USA

[7] School of Interdisciplinary Arts and Sciences, Division of Sciences and Mathematics, University of Washington, Tacoma, 98402, Tacoma, USA

Contents of this file

Introduction

Text S1 includes the detailed description of RHESSys model. Text S2 described the model parameterization and calibration results. Text S3 described the results of how spatial fire regimes respond to beetle outbreaks. Figures S1 to S8 are supplementary figures to support results and discussion. Table S1 summarizes the original and revised conceptual framework of how fire characteristics respond to beetle outbreaks.

Text S1. RHESSys model descriptions

In RHESSys, a watershed is partitioned into a hierarchical set of spatial units: patches, subbasins, and an entire basin. Patches are the smallest spatial unit and the scale at which vertical hydrology and biogeochemistry are modeled. Climate forcing data are organized at the patch level, and vary with elevation, slope, and aspect. Subbasins are closed drainage areas that encompass both sides of a single stream reach. RHESSys uses geospatial data layers, including a digital elevation model (DEM), soil, and landcover maps to characterize biophysical properties across a watershed. It then simulates surface and subsurface flow between patches to generate streamflow (Tague & Band, 2004). Each patch contains a soil and litter layer and multiple canopy layers that include hydrologic, carbon and nutrient state variables. Vertical hydrologic fluxes include canopy interception, throughfall, snow sublimation, snowmelt, infiltration, capillary rise, evaporation from the soil, and litter/canopy transpiration. Vertical subsurface drainage is modelled as a function of hydraulic conductivity, which decays exponentially with soil depth. Lateral subsurface flow is modelled as a function of both hydraulic conductivity and topographic differences between neighboring patches (Tague & Band, 2004).

Hydrological fluxes in RHESSys are tightly coupled with biogeochemical processes. Photosynthesis for overstory and understory canopy layers is modelled using the Farquhar equation (Farquhar & von Caemmerer, 1982), which is constrained by N, light, stomatal conductance, atmospheric carbon dioxide (CO_2) concentrations, and temperature. Growth respiration is calculated as a fixed ratio of new C allocation and is constrained by N concentrations and air temperature using a model developed by Ryan, (1991). Net photosynthate is allocated to roots, stems, and leaves at a daily time step as a function of plant architecture (Dickinson et al., 1998). Soil and litter decomposition are simulated at a daily time step and are constrained by temperature, moisture, and N availability (modified from BIOME-BGC and CENTURY-NGAS; Hanan et al., 2017; Nemani et al., 2005; Parton, 1996). A more detailed description of the RHESSys model can be found by Garcia et al., 2016; Tague & Band, 2004; Tague et al., 2013).

Text S2. Model parameterization

We calibrated six subsurface hydrological parameters in RHESSys: saturated hydraulic conductivity (K_{sat}), decay of K_{sat} with depth (m), air-entry pressure (ϕ_{ae}), pore size index (b), bypass flow to deeper groundwater stores (gw_1), and groundwater drainage rates to the stream (gw_2). The best parameter set was selected by comparing observed and modeled streamflow based on the Nash-Sutcliffe efficiency metric (NSE, to evaluate the peak flow), and percent error in annual flow (to evaluate the total flow). The monthly NSE of streamflow reached 0.94 (an NSE equal to 1 would represent a perfect match), with a percent error of 2.6% (a percent error equal to 0 would represent a perfect match). A detailed description of the model calibration is described by (Ren et al., 2021). To initialize the landscape vegetation, we ran RHESSys-WMFire for 300 years using modified climate data that removed the anthropogenic climate change signal (1900 – 2017, Hanan et al., 2021) and with the fire model "on".

We used LANDFIRE maps (Rollins, 2009) to calibrate and evaluate WMFire model performance in Trail Creek. We selected three criteria: the spatial distribution of fire spread, fire seasonality, and fire return intervals (Hanan et al., 2021). We used simulated fire regimes from 1911 to 2017 for these evaluations. We found that the spatial pattern and seasonality of wildfire generally matched LANDFIRE estimates, and they were not sensitive to the ignition rate (number of ignitions per month). FRI on the other hand was sensitive to the ignition rate. We adjusted the ignition rate based on the watershed area to make the FRI in WMFire generally match LANDFIRE estimates. A more detailed description of WMFire validation for Trail Creek is described by (Hanan et al., 2021).

Text S3. Spatial fire regimes

To understand how fire regime changes across different fuel aridity and fuel loading conditions, we examined how changes in surface fire probability (P_{burn}) caused by beetle outbreaks responded to pre-outbreak fuel loading and fuel aridity. During the red phase, P_{burn} varied mainly in response to changes in fuel loading. Following low beetle-caused mortality (<=20%), increases in P_{burn} were driven by increases in fuel loading that occurred due to the rapid recovery of surviving plants, which dominated over the reduced litter production caused by evergreen tree mortality (e.g., *Figure S1*, mortality 10-20%). Following medium to high beetle-caused mortality (>20%), reduced productivity in evergreen trees dominated over increased productivity of surviving plants, which reduced fuel loading and consequently decreased surface fire probability, especially in arid region of the watershed (*Figure S1*). In the red phase, the effects of beetle-caused mortality level on surface fire probability were similar to the fire size responses (*Figure 4*).

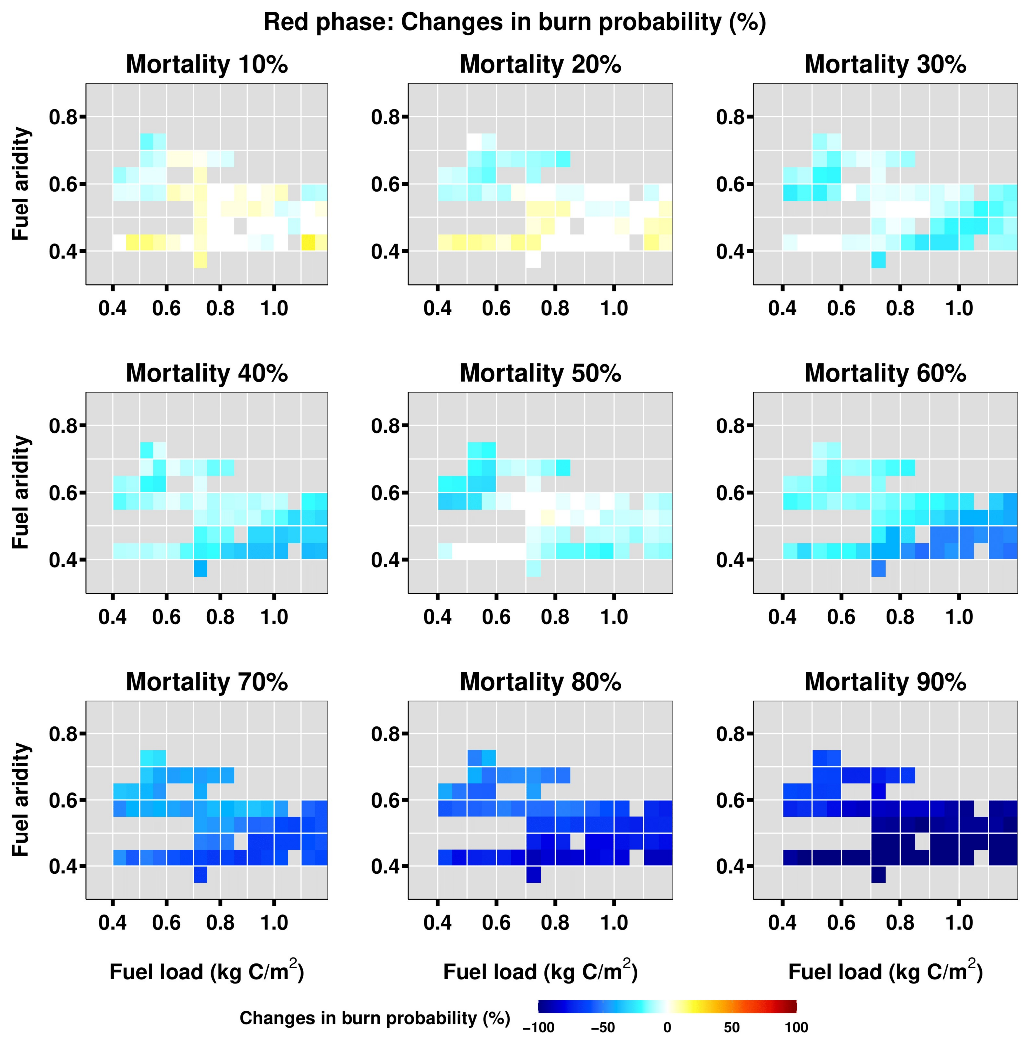

Figure S1. Bivariate plots showing differences in burn probability (between mortality scenarios and the control run) as a function of fuel loading and fuel aridity during the red phase. These plots only include evergreen patches (where beetle outbreaks occurred). Fuel loading and aridity were calculated from the control run, not from the corresponding beetle-caused mortality scenarios. Data are binned at 0.05 increments for both fuel aridity and fuel load and the figure illustrates median changes in surface fire probability (i.e., P_{burn}) for each bin. Warm colors represent an increase in surface fire probability and blue colors represent a decrease.

In the gray phase, P_{burn} generally increased after beetle outbreaks, though the magnitude varied with locations (*Figure S2*). There were two different responses for arid and mesic locations. For relatively mesic locations, which were flammability-limited, P_{burn} increased slightly and was less sensitive to beetle-caused mortality because fire was mostly limited by moisture (*Figure S2*, right side). For the relatively dry forest areas, P_{burn} increased more substantially with increasing beetle-caused mortality because these forests were co-limited by both fuel loading and flammability, and increased fuel loading from snagfall increased P_{burn} (*Figure S2*, left side).

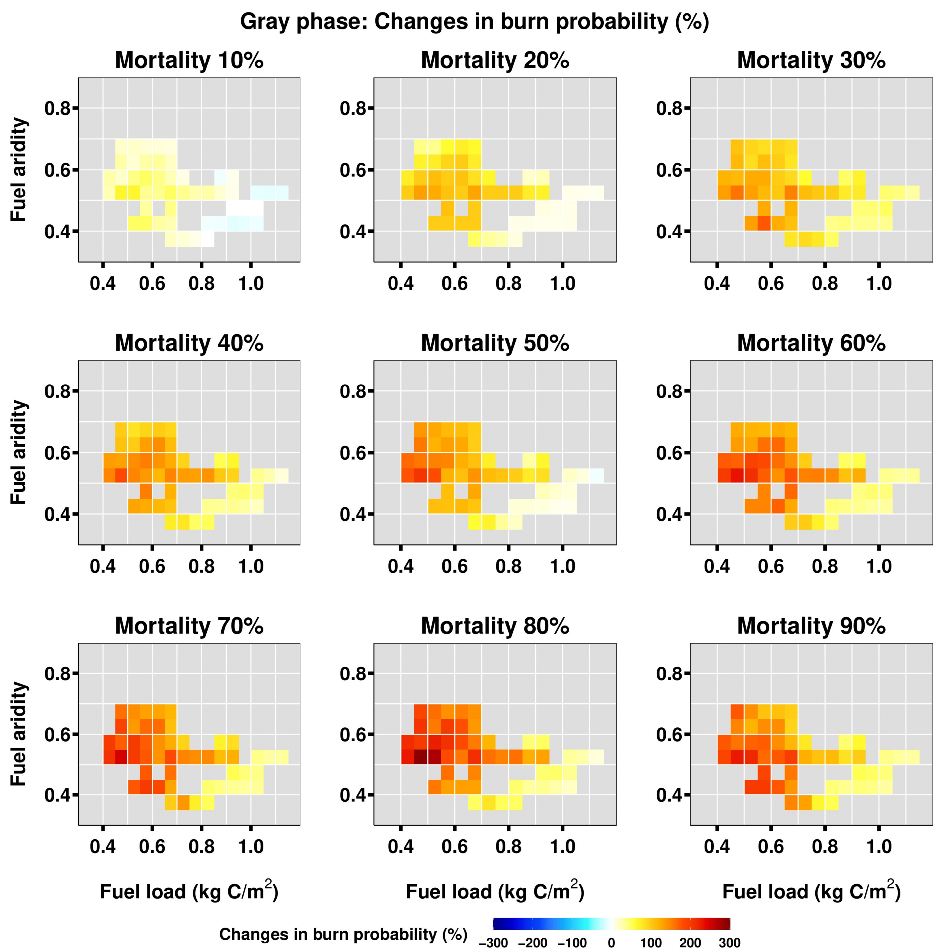

Figure S2. Bivariate plots showing differences in burn probability (between mortality scenarios and the control run) as a function of fuel loading and fuel aridity during the gray phase. These plots only include evergreen patches. Fuel loading and aridity were calculated from the control run, not from the corresponding beetle-caused mortality scenario. Data are binned at 0.05 increments for both fuel aridity and fuel loading, and the figure illustrates median changes in surface fire probability (P_{burn}) for each bin. Warm colors represent an increase in surface fire probability and blue colors represent a decrease.

In the old phase, P_{burn} responded nonlinearly to beetle-caused mortality (*Figure S3*). P_{burn} first increased at low and medium beetle-caused mortality (<=50%), then decreased at high mortality (>50%, *Figure S3*). With greater mortality and more litter loading from snagfall, the previously fuel-limited dry forest areas became flammability-limited and P_{burn} decreased in response to decreasing fuel aridity. These results suggest that after beetle outbreaks, increases in fuel loading can counteract decreases in fuel aridity. Once fuel loading increases enough, fire regimes shift to become flammability-limited.

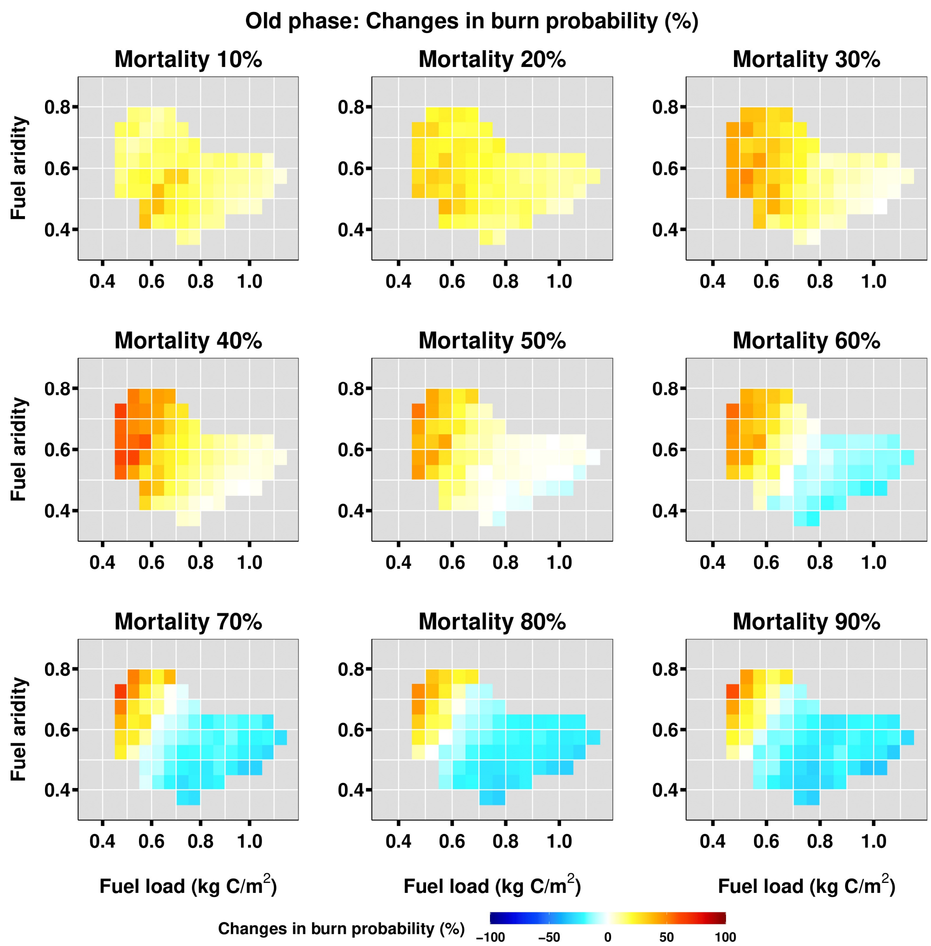

Figure S3. Bivariate plots showing differences in burn probability (between mortality scenarios and the control run) as a function of fuel loading and fuel aridity during the old phase. These plots only include evergreen patches. Fuel loading and aridity were calculated from the control run, not from the corresponding beetle-caused mortality scenario. Data are binned at 0.05 increments for both fuel aridity and fuel load, and the figure illustrates median changes in surface fire probability (P_{burn}) for each bin. Warm colors represent an increase in surface fire probability and blue colors represent a decrease.

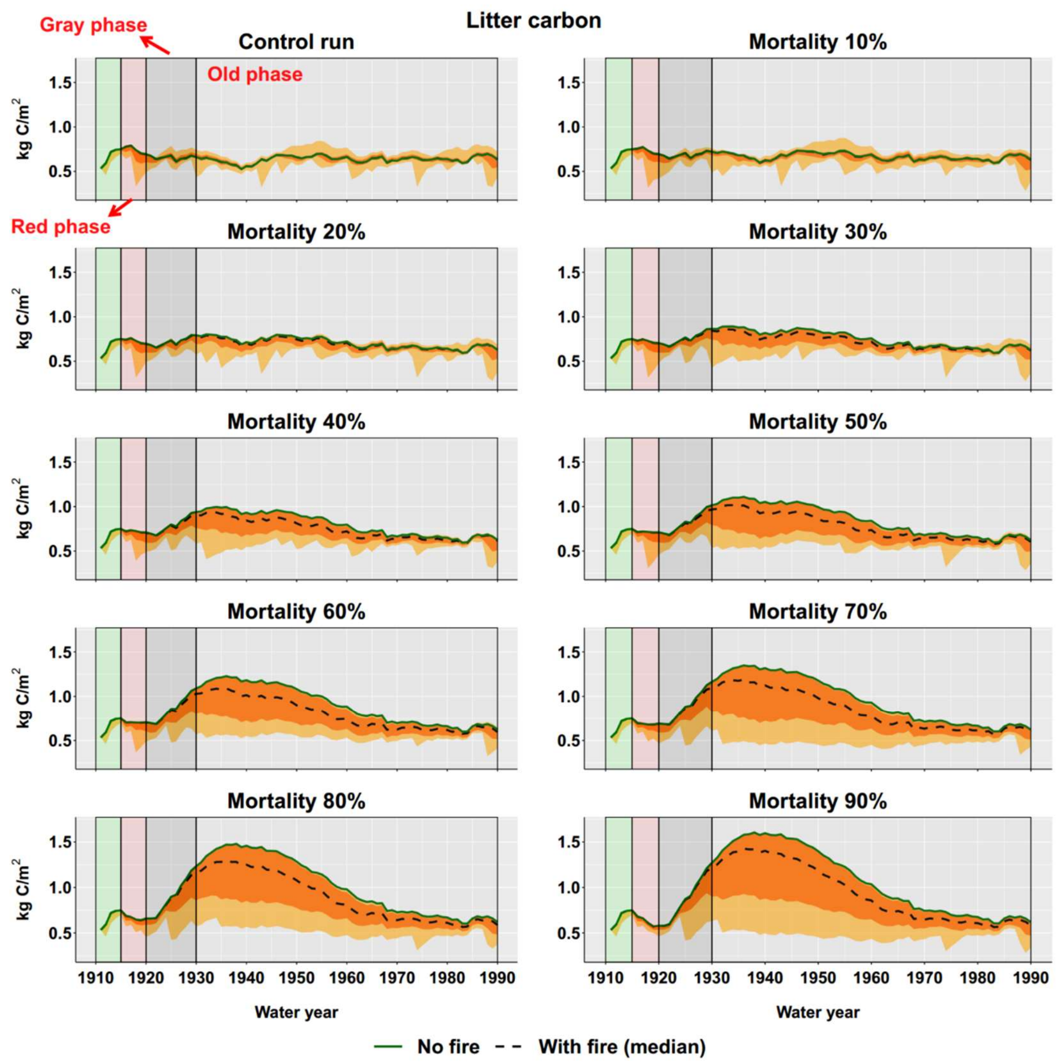

Figure S4. distribution of litter C for the 200 fire simulations and the no fire scenario; the dashed line is the median litter state for the fire scenarios; and the solid green line is the no fire scenario. Orange is maximum and minimum litter C, dark red is 5th and 95th percentile; The differences between the no-fire scenario (green line) and fire scenarios (other lines) can be a surrogate for cumulative fire severity.

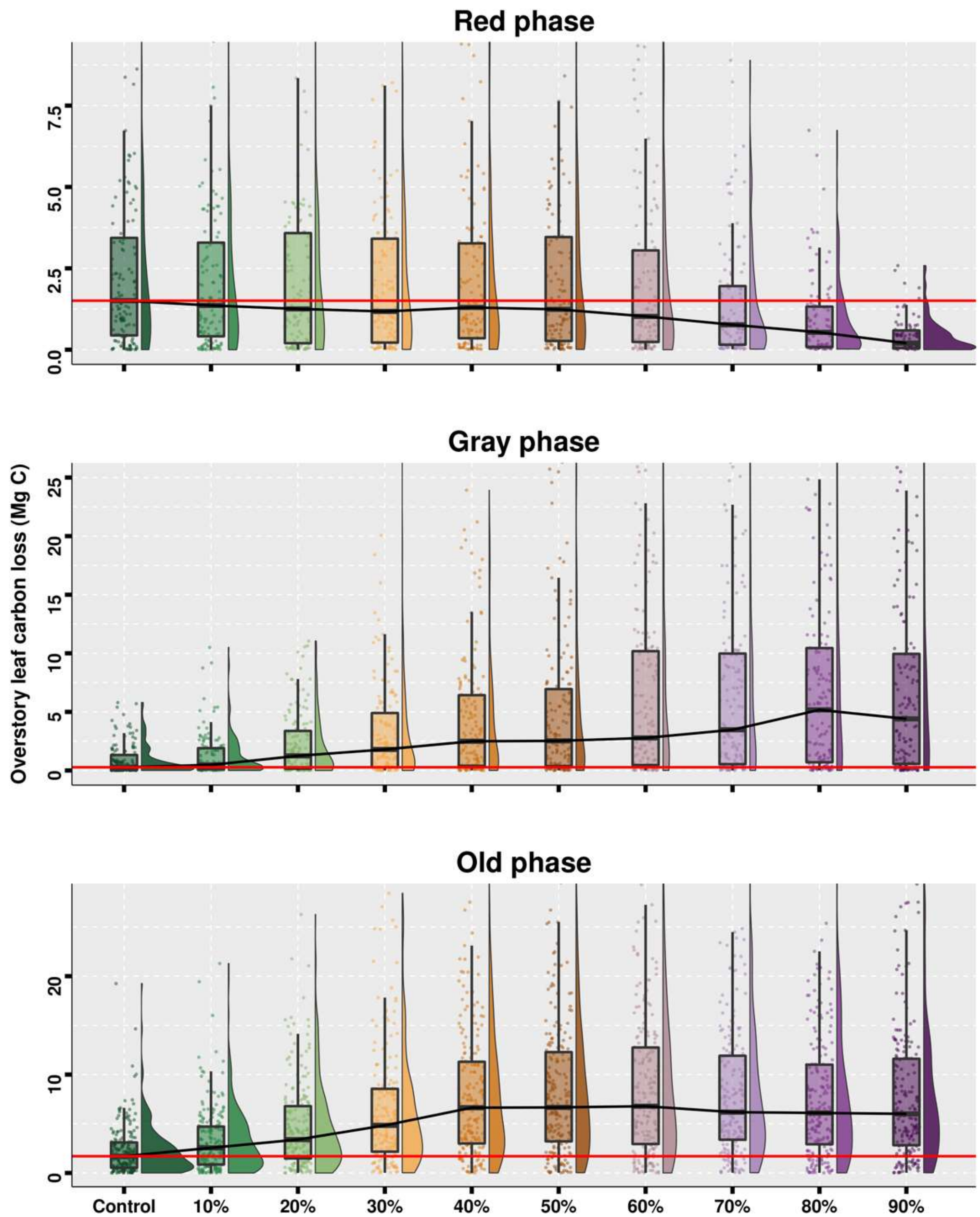

Figure S5. Distribution of overstory canopy fire severity for each phases. Results are distribution of 200 simulation replicates for each scenario. Box plots show 25th, median, and 75th percentile of fine C loss Red line is the median of control run, black line connects the median line of each scenario. Low beetle-caused mortality is 10-20% mortality; medium beetle-caused mortality is 10-50% mortality; and high beetle-caused is larger than 50% mortality. Notice that the y-axis is different for different phases for better showing the extreme fire severity.

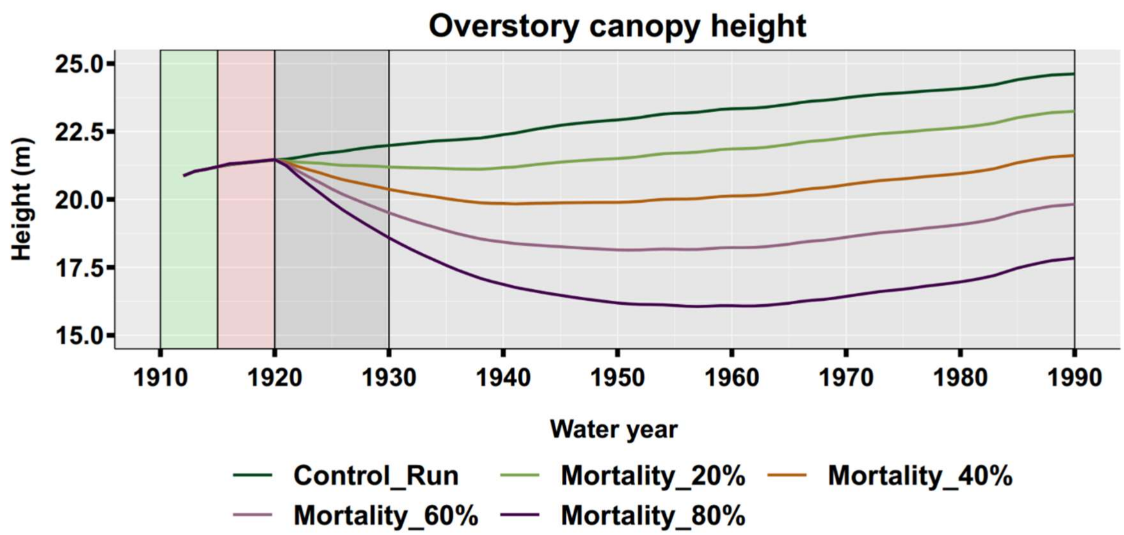

Figure S6. Overstory canopy height for different scenarios. The background colors represent different beetle outbreak phases: pre-outbreak (1910-1915), red phase (1916-1920), gray phase (1921-1930) and old phase (1931-1990).

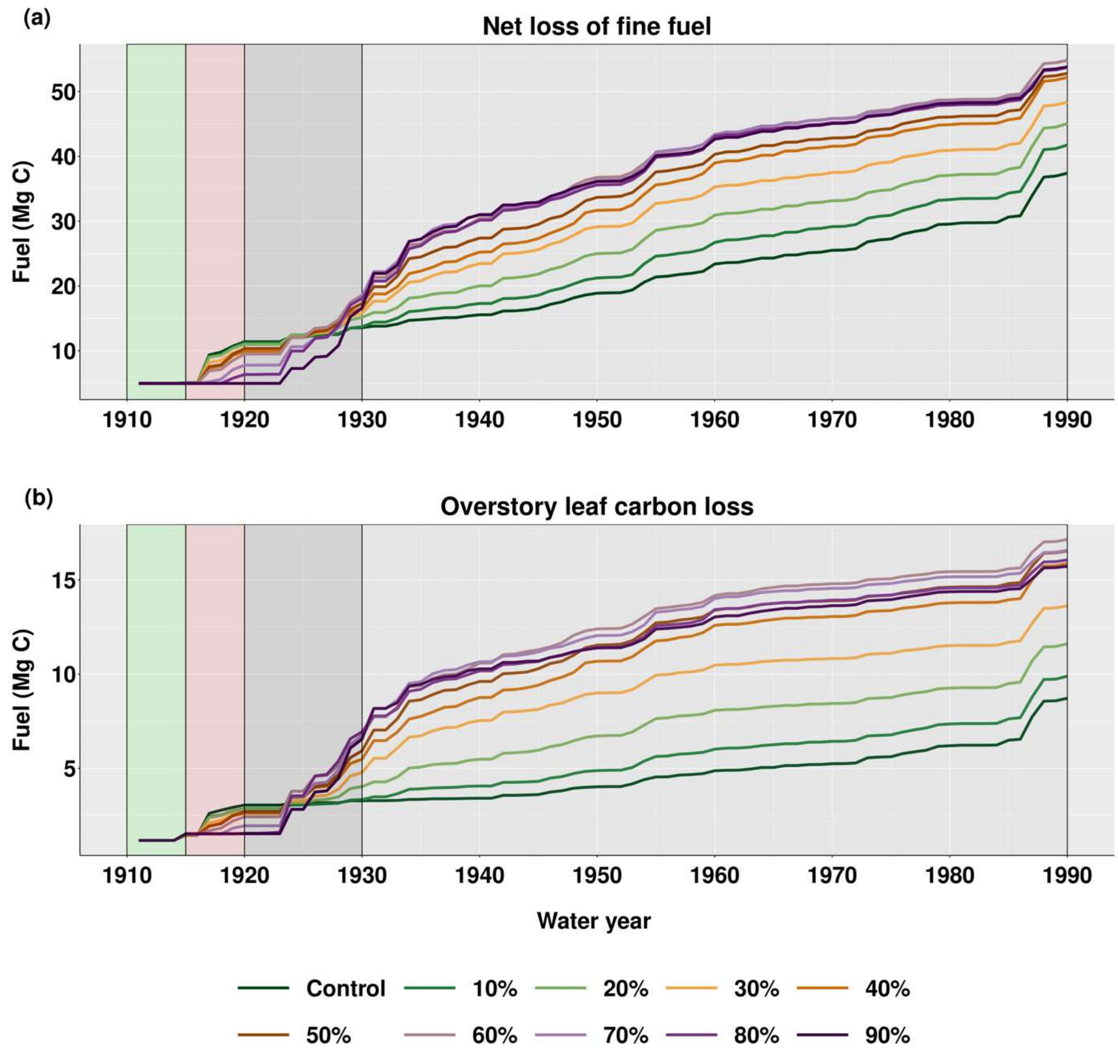

Figure S7. Cumulative fire severity with respect to surface fine fuels (a) and overstory canopy fuels (b) in different phases. The background color indicates pre-outbreak (before 1915), red (1915-1920), gray (1921 – 1930) and old phases (1931 – 1990) of beetle outbreak.

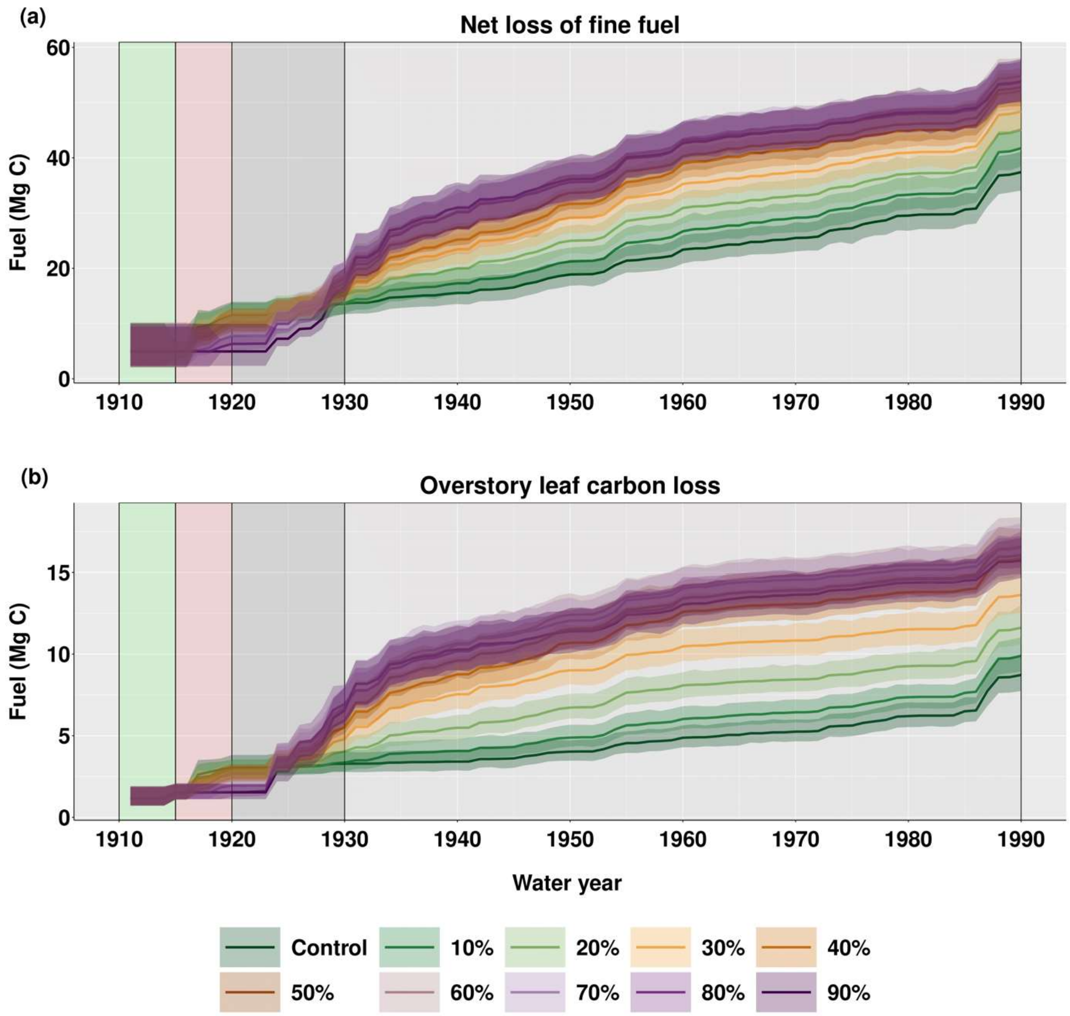

Figure S8. Cumulative fire severity with respect to surface fine fuels (a) and overstory canopy fuels (b) in different phases. we applied a bootstrapping approach to calculate 95% confidence windows for each scenario. The background color indicates pre-outbreak (before 1915), red (1915-1920), gray (1921 – 1930) and old phases (1931 – 1990) of beetle outbreak.

Table S1. Summary of how fire characteristics (surface fire probability, surface fire severity, and crown fire severity) respond to beetle outbreaks in different phases. The blue colored text refers to findings of studies synthesized by (Hicke et al., 2012). *The italic red colored text refers to findings from this research. Content inside parenthesis identify the mechanisms of driving fire responses after beetle outbreaks.*

Fire characteristics	**Red phase**	**Gray phase**	**Old phase**
Surface fire probability	No change (no change in dead surface fuel) *Decrease (decreased fuel loading), more decreases relative to higher beetle-caused mortality level.*	Increase (higher dead surface fuel loading) *Increase (more fuel loading), increase more with higher mortality level, and reach plateau when mortality level larger than 50%.*	Increase (higher dead surface fuel loading) *Decrease at high mortality level (lower fuel aridity); Increase at low to medium mortality level (higher fuel loading).*
Surface fire severity	No change (no change in dead surface fuel) *Decrease (decreased fuel loading), more decreases relative to higher beetle-caused mortality level.*	Increase (higher dead surface fuel loading) *Increase (more fuel loading), increase more with higher mortality level.*	Increase (higher dead surface fuel loading) *Increase (more fuel loading), increase more with higher mortality level, and reach plateau when mortality level larger than 50%.*
Crown fire severity	Increase (reduced foliage moisture) *Decrease (decrease in surface fire intensity), more decreases relative to higher beetle-caused mortality level.*	Lower (reduced canopy bulk density dominates over increased surface fire probability) *Increase (higher surface fire intensity and lower overstory canopy height), increase more with higher mortality level.*	Lower (reduced canopy bulk density dominates over increased surface fire probability) *Increase (higher furface fire probability and lower overstory canopy height), increase more with higher mortality level, and reach plateau when mortality level larger than 50%.*

References

Dickinson, R. E., Shaikh, M., Bryant, R., & Graumlich, L. (1998). Interactive Canopies for a Climate Model. *Journal of Climate*, *11*(11), 2823–2836. https://doi.org/10.1175/1520-0442(1998)011<2823:ICFACM>2.0.CO;2

Farquhar, G. D., & von Caemmerer, S. (1982). Modelling of Photosynthetic Response to Environmental Conditions. In O. L. Lange, P. S. Nobel, C. B. Osmond, & H. Ziegler (Eds.), *Physiological Plant Ecology II: Water Relations and Carbon Assimilation* (pp. 549–587). Berlin, Heidelberg: Springer. https://doi.org/10.1007/978-3-642-68150-9_17

Garcia, E. S., Tague, C. L., & Choate, J. S. (2016). Uncertainty in carbon allocation strategy and ecophysiological parameterization influences on carbon and streamflow estimates for two western US forested watersheds. *Ecological Modelling*, *342*, 19–33. https://doi.org/10.1016/j.ecolmodel.2016.09.021

Hanan, E. J., Tague, C. (Naomi), & Schimel, J. P. (2017). Nitrogen cycling and export in California chaparral: the role of climate in shaping ecosystem responses to fire. *Ecological Monographs*, *87*(1), 76–90. https://doi.org/10.1002/ecm.1234

Hanan, E. J., Tague, C., Choate, J., Liu, M., Kolden, C., & Adam, J. (2018). Accounting for disturbance history in models: using remote sensing to constrain carbon and nitrogen pool spin-up. *Ecological Applications: A Publication of the Ecological Society of America*, *28*(5), 1197–1214. https://doi.org/10.1002/eap.1718

Hanan, E. J., Ren, J., Tague, C. L., Kolden, C. A., Abatzoglou, J. T., Bart, R. R., et al. (2021). How climate change and fire exclusion drive wildfire regimes at actionable scales. *Environmental Research Letters*, *16*(2), 024051. https://doi.org/10.1088/1748-9326/abd78e

Hicke, J. A., Johnson, M. C., Hayes, J. L., & Preisler, H. K. (2012). Effects of bark beetle-caused tree mortality on wildfire. *Forest Ecology and Management*, *271*, 81–90. https://doi.org/10.1016/j.foreco.2012.02.005

Nemani, R. R., Running, S. W., & Thornton, P. E. (2005). *BIOME-BGC: TERRESTRIAL ECOSYSTEM PROCESS MODEL, VERSION 4.1.1*. Retrieved from http://daac.ornl.gov/cgi-bin/dsviewer.pl?ds_id=805

Parton, W. J. (1996). The CENTURY model. In D. S. Powlson, P. Smith, & J. U. Smith (Eds.), *Evaluation of Soil Organic Matter Models* (Vol. 38, pp. 283–291). Springer, Berlin, Heidelberg: Evaluation of Soil Organic Matter Models.

Ren, J., Adam, J. C., Hicke, J. A., Hanan, E. J., Tague, C. L., Liu, M., et al. (2021). How does water yield respond to mountain pine beetle infestation in a semiarid forest? *Hydrology and Earth System Sciences*, *25*(9), 4681–4699. https://doi.org/10.5194/hess-25-4681-2021

Reyes, J. J., Tague, C. L., Evans, R. D., & Adam, J. C. (2017). Assessing the Impact of Parameter Uncertainty on Modeling Grass Biomass Using a Hybrid Carbon Allocation Strategy: A HYBRID CARBON ALLOCATION STRATEGY. *Journal of Advances in Modeling Earth Systems*, *9*(8), 2968–2992. https://doi.org/10.1002/2017MS001022

Rollins, M. G. (2009). LANDFIRE: a nationally consistent vegetation, wildland fire, and fuel assessment. *International Journal of Wildland Fire*, *18*(3), 235–249. https://doi.org/10.1071/WF08088

Ryan, M. G. (1991). Effects of Climate Change on Plant Respiration. *Ecological Applications*, *1*(2), 157–167. https://doi.org/10.2307/1941808

Tague, C. L., & Band, L. E. (2004). RHESSys: Regional Hydro-Ecologic Simulation System—An Object-Oriented Approach to Spatially Distributed Modeling of Carbon, Water, and

Nutrient Cycling. *Earth Interactions*, *8*(19), 1–42. https://doi.org/10.1175/1087-3562(2004)8<1:RRHSSO>2.0.CO;2

Tague, Christina L., McDowell, N. G., & Allen, C. D. (2013). An Integrated Model of Environmental Effects on Growth, Carbohydrate Balance, and Mortality of Pinus ponderosa Forests in the Southern Rocky Mountains. *PLOS ONE*, *8*(11), e80286. https://doi.org/10.1371/journal.pone.0080286